UNITED STATES DEPARTMENT OF THE INTERIOR

GEOLOGICAL SURVEY

Crustal structure of Southwestern Saudi Arabia

by

M. E. Gettings, H. R. Blank, W. D. Mooney 1/,

and J. H. Healy 1/

Open-File Report 83-638

Prepared for Ministry of Petroleum and Mineral Resources,
Deputy Ministry for Mineral Resources
Jiddah, Kingdom of Saudi Arabia

This report is preliminary and has not been reviewed for conformity with U.S. Geological Survey editorial standards and stratigraphic nomenclature.

1/ U.S. Geological Survey, Menlo Park, California

1983

CONTENTS

ILLUSTRATIONS

CRUSTAL STRUCTURE OF SOUTHWESTERN SAUDI ARABIA

by

M. E. Gettings, H. R. Blank, W. D. Mooney[1]/,

and J. H. Healy[1]/

ABSTRACT

The southwestern Arabian Shield is composed of uplifted Proterozoic metamorphic and plutonic rocks. The Shield is bordered on the southwest by Cenozoic sedimentary and igneous rocks of the Red Sea paar and on the east by the Arabian Platform, an area of basin sedimentation throughout Phanerozoic time. The Shield appears to have been formed by successive episodes of island arc volcanism and sea-floor spreading, followed by several cycles of compressive tectonism and metamorphism. An interpretation and synthesis of a deep-refraction seismic profile from the Riyadh area to the Farasan Islands, and regional gravity, aeromagnetic, heat flow, and surface geologic data have yielded a self-consistent regional-scale model of the crust and upper mantle for this area.

The model consists of two 20 km-thick layers of crust with an average compressional wave velocity in the upper crust of about 6.3 km/s and an average velocity in the lower crust of about 7.0 km/s. This crust thins abruptly to less than 20 km near the southwestern end of the profile where Precambrian outcrops abut the Cenozoic rocks and to 8 km beneath the Farasan Islands. The data over the coastal plain and Red Sea shelf areas are fit satisfactorily by an oceanic crustal model. A major lateral velocity inhomogeneity in the crust is inferred about 25 km northeast of Sabhah and is supported by surface geologic evidence.

The major velocity discontinuities occur at about the same depth across the entire Shield and are interpreted to indicate horizontal metamorphic stratification of the Precambrian crust. Several lateral inhomogenities in both the upper and lower crust of the Shield are interpreted to indicate bulk compositional variations.

The subcrustal portion of the model is composed of a hot, low-density lithosphere beneath the Red Sea which is systematically cooler and denser to the northeast. This model provides a mechanism which explains the observed topographic

---

[1]/ U.S. Geological Survey, Menlo Park, California

uplift, regional gravity pattern, heat flow, and mantle compressional wave velocities. Such a lithosphere could be produced by upwelling of hot asthenosphere beneath the Red Sea which then flows laterally beneath the lithosphere of the Arabian Plate.

INTRODUCTION

The major geologic province of western Saudi Arabia is a Precambrian Shield bordered on the east by a platform of gently dipping Cambrian and younger sedimentary rocks and on the west by rocks of the Tertiary Red Sea paar. During the past 8 years geophysical data have been collected or compiled at a regional scale along a 150-km-wide transect from the platform across the southern part of the Arabian Shield and into the Red Sea paar. A crustal section for southwestern Saudi Arabia has been constructed from an integrated study of these data and constrained by surface geological relations. Previous to this work, knowledge of the crustal structure of the Arabian Shield was limited to inference from surface geologic mapping (see, for example, Schmidt and others, 1978), geochemical and isotopic studies (Stacey and others, 1981), and studies of Rayleigh waves from earthquakes (Niazi, 1968; Knopoff and Fouda, 1975).

The geophysical transect (fig. 1), extending from near Riyadh to the Farasan Islands in the southwest, includes aeromagnetic data (Andreasen and others, 1980), regional gravity data (Gettings, 1983), seismic deep-refraction data (Blank and others, 1979; Healy and others, 1983), heat flow observations (Gettings and Showail, 1982), and regional-scale geologic information (U.S. Geological Survey-Arabian American Oil Company, 1963; Brown, 1972).

The refraction profile extends for about 1,000 km, approximately down the center of the transect; it parallels the southeastern boundary of the Arabian Shield and is nearly perpendicular to other first-order structural boundaries (fig. 1). Starting on the Arabian Platform west of Riyadh, it traverses the Al Amar-Idsas fault zone, the Shammar, Najd, and Hijaz-Asir tectonic provinces (Greenwood and others, 1977), the exposed western margin of the continental plate at the foot of the Hijaz-Asir escarpment, and almost all of the eastern Red Sea shelf, from coastal plain to axial trough in the southern Red Sea.

For the refraction profile, we were primarily seeking regional information on the thickness, structure, and bulk composition of crustal layers to the depth of the Mohorovicic discontinuity (40 km or more), which could then be correlated with geologic and other geophysical data. The objective of the geophysical transect program was to examine fundamental questions concerning the late Proterozoic cratonization and

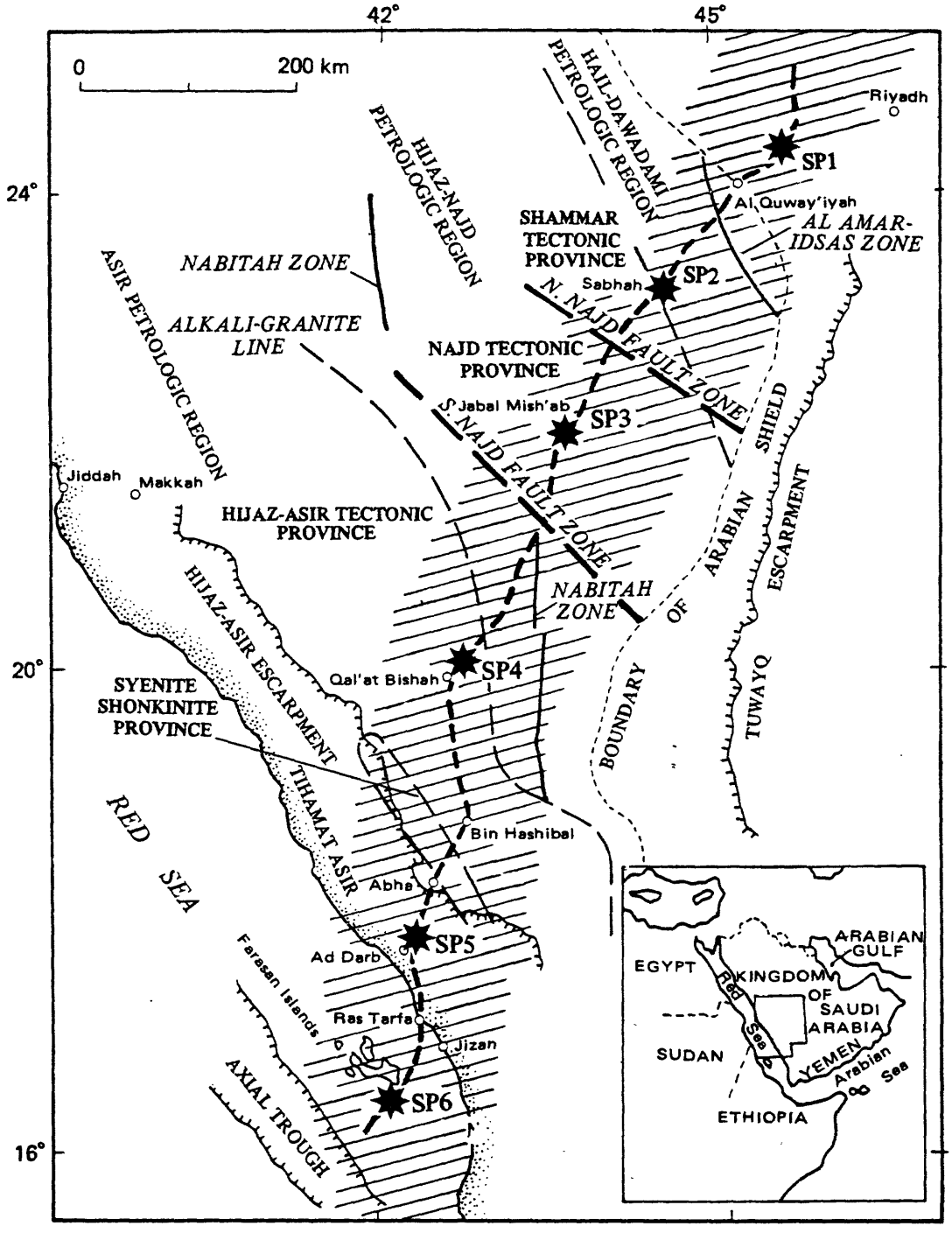

Figure 1.--Index map showing the location of the southwestern Saudi Arabian geophysical transect (hachured) and seismic deep-refraction line (heavy dashed line). Physiographic, geographic, tectonic, and petrologic features are also shown. Shot points of the 1978 seismic refraction line are shown as SP1, SP2...

tectonic evolution of the Arabian Shield, the origin and significance of tectonic, magmatic, and metallogenic provinces of the Shield, and the nature of a continental plate margin in an active spreading zone.

In this paper, we proceed from a brief geologic summary followed by a discussion of the crustal section derived mainly from the seismic refraction data. We then examine the implications of the gravity, aeromagnetic, and heat flow data sets upon the inferred crustal structure. Finally, we summarize our crustal model for southwestern Saudi Arabia and speculate on upper mantle processes that may be active. The work on which this report is based was conducted as part of an agreement between the Saudi Arabian Ministry of Petroleum and Mineral Resources and the U.S. Geological Survey.

GEOLOGIC SETTING

Most of the transect traverses the Arabian Shield (fig. 2), which consists predominantly of Precambrian metamorphic and plutonic rocks and forms the western one-third of the Arabian Peninsula. The Shield is thought to have evolved from island arcs that formed during a series of subduction episodes and that were subsequently juxtaposed by compressional orogenies (Schmidt and others, 1978). To the east, the Shield is bounded by the Mesozoic sedimentary rocks of the Phanerozoic Arabian Platform, which dip gently eastward and onlap unconformably upon the Shield (Powers and others, 1966). To the west, the Shield abuts the Tertiary rocks at the eastern edge of the Red Sea sea-floor spreading system. This tectonic boundary is characterized by complex faulting and Tertiary dike injections and volcanism.

Arabian Platform

Powers and others (1966) have summarized the sedimentary geology of the Arabian Peninsula and the 1:2,000,000-scale Geologic Map of the Arabian Peninsula (U.S. Geological Survey-Arabian American Oil Company, 1963) shows the geologic field relations. Most of the following discussion is derived from the report of Powers and others (1966).

The extreme northeastern end of the seismic refraction line is situated in the Jurassic Dhruma Formation, which is predominantly limestone and shale. Proceeding southwest, the line crosses the exposed strata of the eastward-dipping sequence of Marrat Formation shale and limestone (Lower Jurassic), an unconformity, the Minjur Sandstone (Lower Jurassic or Triassic), the Jilh Formation sandstone and limestone (Triassic), and the Sudair Shale (Lower Triassic or Permian) at shot point 1. Continuing southwest, the refraction line crosses the Upper Permian Khuff Formation limestone and shale, which is the base of the sedimentary sequence in this

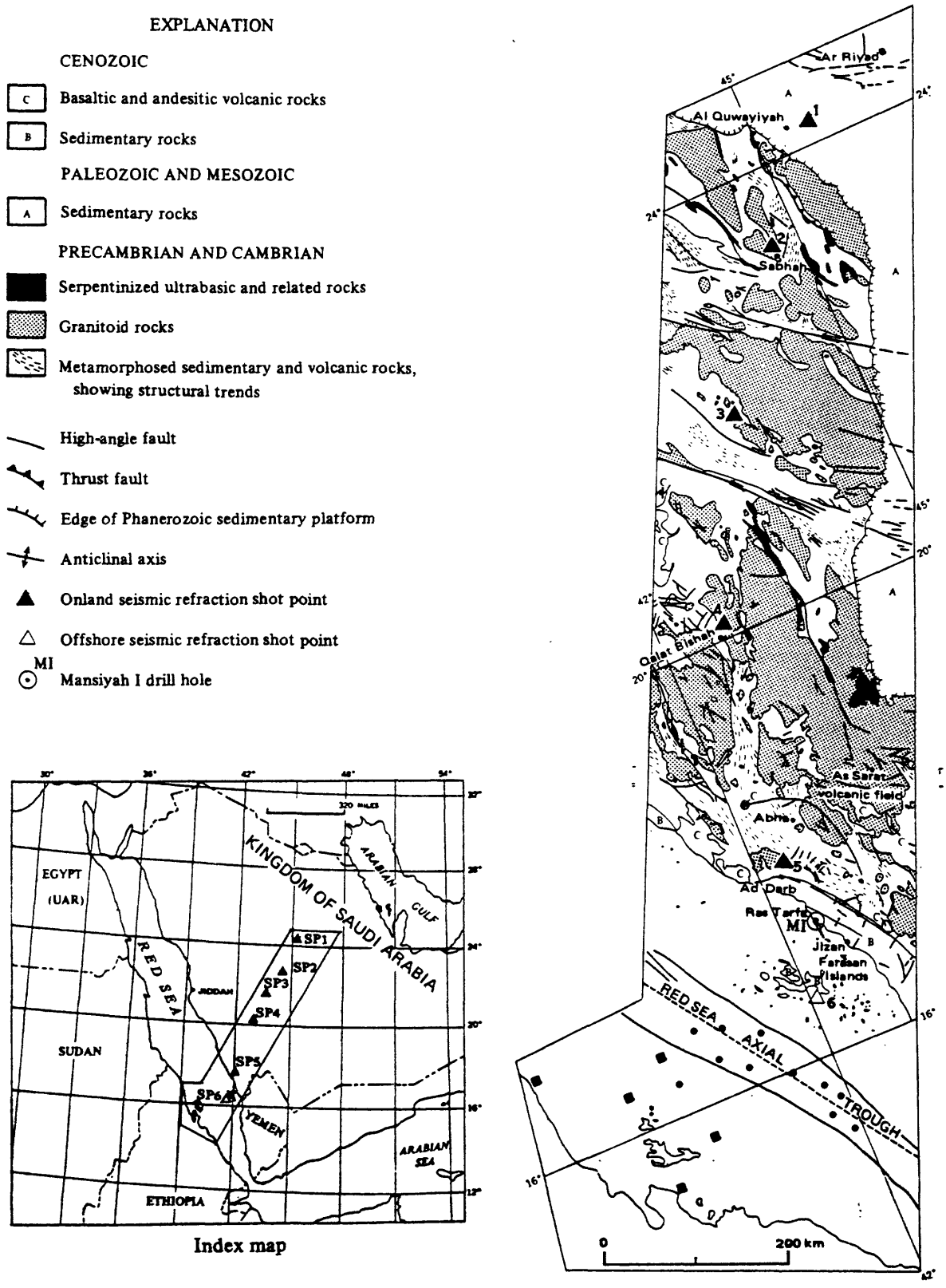

Figure 2.--Generalized geologic map of the geophysical transect. Geologic data are from Brown (1972). Heat flow measurement sites on the Red Sea shelf (solid squares) and Red Sea axial trough (solid circles) are from Girdler and Evans (1977). Dashed line in Red Sea is an arbitrarily defined axis of the deep-water trough, chosen as a single straight line through the deepest water south of the latitude 20° N.

locality, lying unconformably on the metamorphic rocks of the Shield (Powers and others, 1966; figs. 1 and 2, this paper).

The sedimentary rocks dip very gently and uniformly to the east-northeast, from about one degree at the base of the section to about 0.3° in the Upper Cretaceous and Eocene rocks. The decrease of dip with decreasing age indicates gradual subsidence continuously from Cambrian to Eocene time (Powers and others, 1966). This area, called the Interior Homocline by Powers and others (1966), has two parts: one to the north of Riyadh where the strike is to the northwest, and the other south of Riyadh where the strike is to the southwest. The separating structure, known as the Central Arabian Arch, trends approximately east-west and has a complex history of epirogenic movement in the Paleozoic and early Mesozoic. During the Middle Cretaceous, the arch became a flexure zone between a region of uplift to the south and a region of subsidence to the north. During the Paleocene and Eocene, subsidence continued in the north, and began in the south, forming the Rub al Khali basin. The line of recorder stations begins at the northern side of the arch, and crosses the arch structure to the west of its main fault and graben system (fig. 2).

Arabian Shield

The Arabian Shield is a stable craton of predominantly late Precambrian metavolcanic, metasedimentary, and plutonic rocks having an area of about 770,000 km^2. The exposed surface is composed of approximately 50 percent plutonic rocks and 50 percent volcanic and sedimentary rocks; among the plutonic rocks, about 70 percent are granitoid. The Shield has undergone several cycles of metamorphism, tectonism, and plutonism whose intensity was areally quite variable. Here we briefly describe the major tectonic, petrologic, and structural/lithologic provinces and regions that may relate to the regional variations in crustal structure of the Arabian Shield. More detailed descriptions of the general geology of all or parts of the Arabian Shield may be found in Brown and Jackson (1960), Brown (1972), Schmidt and others (1973), Greenwood and others (1977), Brown and Jackson (1978), Schmidt and others (1978), and Hadley and Schmidt (1979), among others. The major geochronologic relationships are given in Baubron and others (1976), Fleck and others (1976), Aldrich and others (1978), Cooper and others (1979), Fleck and others (1979), and Stacey and others (1981). The generalized history of the development of the Shield is summarized by Schmidt and others (1978), from whom we quote here (see fig. 1 for place names).

"The Arabian Shield was formed by successive accretions of newly formed crust between 1,000 and 700 Ma ago. Successively younger island arcs formed to the east as west-dipping

subduction zones shifted eastward. West of Bishah, the volcanic-plutonic crust had consolidated against Africa by about 780 Ma ago when westward-directed subduction ceased at the Nabitah suture.

"A new marginal island arc formed subsequently east of Bishah in the southern Najd, and subduction was renewed at the Idsas suture in the eastern Najd. The volcanic arc consisted of calc-alkaline volcanic rocks (Halaban group), dominantly andesite but ranging from basalt to dacite, and comagmatic, subvolcanic plutonic rocks, dominantly diorite but ranging from gabbro to trondhjemite. About 725 Ma ago this primitive crust was thickened by large intermediate-depth plutons of hornblende tonalite and mafic granodiorite. Compressive tectonism produced folds and faults of northerly trends and was accompanied by greenschist facies metamorphism.

"A continental collision occurred east of the Najd province about 625 Ma ago and initiated extensive compressional orogeny and potassic granite plutonism throughout the Shield. Large, syntectonic batholiths of calc-alkaline, leucocratic, biotite granodiorite-monzogranite formed the cores of large north-trending gneiss domes that were asymmetric toward the west. The domes consist of tonalitic and granodioritic orthogneiss that represents the low-density, plutonic part of the earlier Halaban crust. Strong compression resulted in northerly-trending structures including large west-directed thrust faults.

"Posttectonic, diapiric plutons of granite and alkalic granite intruded the eroding crust at progressively shallower levels until about 600 Ma ago. Molasse deposits of the Murdama group transgressed westward across the eroding crust and were subsequently deformed along northerly trends. Renewed compression of the now thick continental crust resulted in large, northwest-trending Najd faults that have left-lateral displacements aggregating 300 km. The Najd faulting terminated about 560 Ma ago. Transgressive, quartzose sandstone of early Paleozoic age subsequently covered the stabilized craton."

Greenwood and others (1977) and Schmidt and others (1978) have divided the southern Arabian Shield in this area into several tectonic provinces. The region that extends from the exposures of Phanerozoic sedimentary rock to approximately midway between shot points 2 and 3 (fig. 1) is designated the Shammar tectonic province. It is underlain by late-tectonic, calc-alkaline granitic rocks and extrusive equivalents, and metamorphosed sedimentary and volcanic rocks of the greenschist facies (Brown, 1972). The Idsas suture zone, which is marked by the trace of the Al Amar-Idsas thrust fault (Schmidt and others, 1978), extends north-northwest in an arc

that is truncated at both ends at the boundary of the Shield. The thrust block to the northeast of the fault has been interpreted as the western edge of an allochthonous continental crust sutured to the remainder of the Shield along the Idsas zone. Evidence from lead isotope studies of mineralized zones in this area suggests that this area may be underlain by much older crust of about 2100 Ma in age (Stacey and others, 1981).

The Shammar tectonic province is bounded on the southwest by the Najd tectonic province (fig. 1). These provinces are separated by the southern limit of the northern Najd fault zone, an area of extensive left-lateral strike-slip faulting. This fault zone trends northwest and is about 60 km wide, spreading toward the north to a width of about 90 km at the northwestern edge of the transect (fig. 2). The Najd tectonic province continues as a broad, northwest-trending belt to about midway between shot points 3 and 4. The province is characterized by large amounts of syntectonic granites that have intruded predominantly andesitic metavolcanic and metasedimentary greenstones and greenschists (Brown, 1972; Schmidt and others, 1978). Ubiquitous faulting, tectonism, and extensive intrusion of mafic dike material also characterize this province.

The Najd province is bordered on the southwest by the Hijaz-Asir tectonic province from which it is separated by the southern Najd fault zone. This province, which extends to the Hijaz-Asir escarpment, is not severely affected by tectonism. It is composed of several north-trending subprovinces, or belts. The rocks of the most northeastern zone are serpentinized ultramafic ones and the belt is designated the Nabitah fault or suture zone by Schmidt and others (1978). The Nabitah zone has been interpreted by them as the expression of a Precambrian subduction zone. To the west, a belt of asymmetric gneiss domes is thought to be the crust of a marginal basin that was compressed and folded into nappe structures by a colliding crustal plate during a subsequent sea-floor-spreading episode to the east (Schmidt and others, 1978).

The gneiss dome belt terminates approximately 40 km southwest of Bishah against a belt of metavolcanic and metasedimentary rock, predominantly andesitic to basaltic in composition and increasing in age and proportion of basalt toward the west. Schmidt and others (1978) believed that these rocks represent the oldest of the island arcs forming the Shield and have the most primitive composition. They are, in some cases, severely deformed, are metamorphosed to varying degrees, and are intruded by granitoid batholiths of pretectonic age.

Stoeser and Elliott (1979) have defined petrologic regions of the Shield on the basis of the composition and proportions of granitoid rocks. A boundary (fig. 1) trending north-northwest about 30 km southwest of shot point 2 and following the northern limits of the northern Najd fault zone (fig. 2) separates the Hail-Dawadami region, an area where the dominant rock-type is granite, from the Hijaz-Najd region. The Hijaz-Najd region, a broad, northwest-trending area characterized by the presence of alkali granites has as its southwestern boundary the alkali-granite line (Stoeser and Elliott, 1979) that crosses the refraction profile near shot point 4.

The remaining petrologic region, the Asir region (Stoeser and Elliott, 1979, fig. 1), lies between the alkali-granite line and the western edge of the Shield. No alkali granites have been found in it, and calc-alkaline granites are sparse. A narrow, linear belt of syenite and shonkinite intrusives parallel to the Red Sea, the syenite-shonkinite province, crosses the refraction profile approximately at Abha.

Ramsay and others (1979) have defined a series of structural/lithologic provinces of the Arabian Shield along a geotraverse that coincides with a portion of the seismic refraction line. These provinces comprise a mixture of lithologies and metamorphic grades that probably will not exhibit large physical property contrasts. Thus, these provinces probably will not be well discriminated by the geophysical data available for this study, although for other detailed geophysical studies, these provinces will certainly be useful.

The Red Sea and continental margin

It is accepted that the narrow, central axial trough of the Red Sea is an axis of sea-floor spreading associated with the separation of Arabia from Africa (Vine, 1966; McKenzie and others, 1970; Lowell and Genik, 1972; Girdler and Styles, 1974; Le Pichon and Francheteau, 1978). Axial magnetic anomalies indicate that new oceanic crust has been forming for approximately the last 4 to 5 Ma at a sea-floor spreading half-rate of about 1 cm/yr (Vine, 1966; Phillips, 1970; Roeser, 1975; Noy, 1978; Hall, 1980).

For the portion of the Red Sea between latitudes 16° N. and 17° N. (the latitude of the seismic refraction profile line), the eastern margin of the axial trough is a steep submarine escarpment, and all of the main trough to the east is above the 100-fathom bathymetric contour (see Laughton, 1970). The seaward portion of the main trough in this region will be referred to as the "shelf" and the landward portion as the "Tihamat-Asir," which is the formal geographic name of the coastal plain of southwestern Saudi Arabia. The term

"Red Sea rift" will be used where we wish to indicate that portion of the Red Sea structural depression floored mainly by sialic crust and formed prior to continental separation by sea-floor spreading.

The nature of the crust beneath the main trough is not yet established unequivocally. Consequently, the total amount of separation between Arabia and Africa remains a matter of debate. The remarkably close fit of opposing shorelines strongly suggests that nearly the entire width of the Red Sea is due to crustal separation (for example, see Wegener, 1920). This venerable concept is now reinforced by palinspastic reconstructions of Precambrian structures across the Red Sea (Abdel-Gawad, 1970; Greenwood and Anderson, 1977), by stratigraphic and physiographic evidence for 105 km of post-Cretaceous sinistral shear on the Dead Sea rift (Quennell, 1958; Freund and others, 1968, 1970), and by compelling geophysical evidence from magnetic anomalies (Girdler and Styles, 1974).

Both Late Proterozoic rocks and the younger, covering rocks of the Shield margin at the eastern edge of the Tihamat-Asir have been invaded by closely-spaced diabase dikes, and faulted into narrow northwest-trending, west-dipping tectonic slices. The number of dikes and the dike/host volume ratio both increase from east to west across the Shield margin and westernmost exposures consist entirely of sheeted dikes, pillow lavas, and volcaniclastic rocks. Masses of gabbro and granophyre or related rocks intrude the dike complex. The entire assemblage has close petrochemical affinities with oceanic tholeiite. Ghent and others (1980) and Blank (1977) consider the exposed western edge of the Shield to mark the oceanic-continental crustal boundary, principally on the basis of gravity data presented by Gettings (1977). These authors interpret lateral offsets of the dike swarm as Tertiary transform faults. Thus, the region to the west of the Shield margin in southwestern Saudi Arabia should be floored by mafic crust of Tertiary age, and the total opening of the Red Sea at this latitude probably exceeds 350 km (Arabian Shield margin to western shore of the Red Sea at the northern tip of Danakil, Ethiopia). Linear magnetic anomalies, which Gettings (1977), Hall and others (1976), Hall (1980), and Blank and others (1981) infer to have resulted from sea-floor spreading processes, substantiate the Tertiary age and 350-km-wide opening at this latitude.

The chronology of the development of the Red Sea rift is still being deciphered. Linear magnetic anomalies over the shelves of the southern Red Sea have been interpreted as evidence of sea-floor spreading in Eocene-Oligocene time (Girdler and Styles, 1974) or Oligocene-Miocene time (Blank, 1977; Hall and others, 1976; Hall, 1980). Alternatively, the crust may have attenuated in the embryonic rift system. Widespread

flood-basalt volcanism on the margins of the Red Sea apparently began about 29 to 30 Ma ago (Late Oligocene). In southwestern Saudi Arabia, the As Sarat plateau basalts at the edge of the Hijaz-Asir escarpment have been dated at 29 to 24 Ma (Brown, 1970). The layered gabbro and granophyre on the Tihamat-Asir is 22 + 2 Ma old, that is, early Miocene (Coleman and others, 1972). Recent studies of offsets of 18 to 22 Ma-old diabasic dikes on the Levant shear system (Bartov and others, 1980) indicate that most of the sinistral movement of the Sinai Plate relative to the Arabian Plate is accounted for by those offsets. This strongly supports an age of less than 22 Ma for most of the Red Sea crustal extension.

GEOPHYSICAL DATA

Seismic deep-refraction profile

In February 1978 a seismic deep-refraction profile was recorded by the U.S. Geological Survey along a line 1000 km long across the Arabian Shield in western Saudi Arabia (Healy and others, 1983). The line begins in Mesozoic cover rocks near Riyadh on the Arabian Platform, leads southwesterly across three major Precambrian tectonic provinces, traverses Cenozoic rocks of the coastal plain (Tihamat-Asir), near Jizan and terminates at the outer edge of the Farasan Bank in the southern Red Sea. More than 500 surveyed recording sites were occupied, including 19 in the Farasan Islands; the average spacing between recorder sites was about 2 km. Six shot points were used: five on land, with most charges placed below the water table in drill holes, and one at sea, with charges placed on the sea floor and detonated from a ship. Slightly more than 61 metric tons of explosives were used in 19 discrete firings.

Seismic energy was recorded by 100 newly-developed portable seismic stations deployed in approximately 200 km-long arrays for each firing. Each station consisted of a standard 2-Hz vertical component geophone coupled to a self-contained analog recording instrument equipped with a magnetic-tape cassette.

The final seismogram data are on digital magnetic tapes and plotted record sections for each shot point. Record sections include a normalized set of seismograms, reduced at 6 km/s, and a true-amplitude set, reduced at 8 km/s, which have been adjusted for amplifier gain, individual shot size, and distance from the shot point. A detailed description of instruments, field procedures, record sections and travel time interpretation is given in Healy and others (1983).

We used two-dimensional ray-tracing techniques in the data analysis, and our interpretation is based primarily on horizontally layered models. Figure 3 shows the simplest

internally-consistent model of the crust and upper mantle sampled by the profile that we have been able to derive from our analysis.

The Arabian Shield is composed, to first-order, of two layers, each about 20 km thick, with average velocities of about 6.3 km/s and 7.0 km/s, respectively. The crust thins rapidly to less than 20 km total thickness at the western Shield margin, beyond which the Red sea shelf and coastal plain are interpreted to be underlain by oceanic crust.

A major lateral velocity inhomogeneity in the crust northeast of Sabhah in the Shammar tectonic province is interpreted as the suture zone between crustal blocks of different composition. Several high-velocity anomalies in the upper crust correlate with gneiss-dome structures mapped on the surface. Two intra-crustal reflectors at 13 km depth are interpreted as the tops of mafic intrusive zones.

The Mohorovicic discontinuity beneath the Shield rises from 43 km depth in the northeast with 8.2 km/s mantle velocity to 38 km in the southwest with 8.0 km/s mantle velocity. This difference in depth corresponds to the 5 km of basement uplift postulated for the Sinai Peninsula at the Red Sea on the basis of fission track dating (Kohn and Eyal, 1981). Two velocity discontinuities are identified in the upper mantle, at 59 and 70 km depth.

Five representative velocity-depth functions from the interpreted crustal section are plotted in the lower part of figure 3. The southwesternmost plot, near shot point 6, compares favorably with the measured velocity data for the Samail ophiolite in Oman (Christensen and Smewing, 1981). Both velocities and thicknesses compare well except that velocities in the lower crustal layer are in the lower part of the range of measurements.

The two velocity-depth functions near shot point 4 are representative of the Precambrian crust southwest of the Nabitah zone (fig. 3). These functions are in good agreement with the velocity-depth function proposed for the lower crust at the Ivrea zone in northern Italy from laboratory velocity determinations (Fountain, 1976). Based on surface geologic relations (Schmidt and others, 1978), analysis of the long-wavelength components of the gravity and magnetic fields (see below) and the nearly constant depths of the horizontal seismic boundaries, we infer that the crust of the Shield is made up of three layers defined by metamorphic grade, as follows: The upper layer of the crust is interpreted to be rocks of the greenschist facies, amphibolite facies rocks form the intermediate layer, and the lower layer is made up of granulite facies rocks. In the portion of the crust southwest of the Nabitah zone, we infer a mafic composition and a crustal

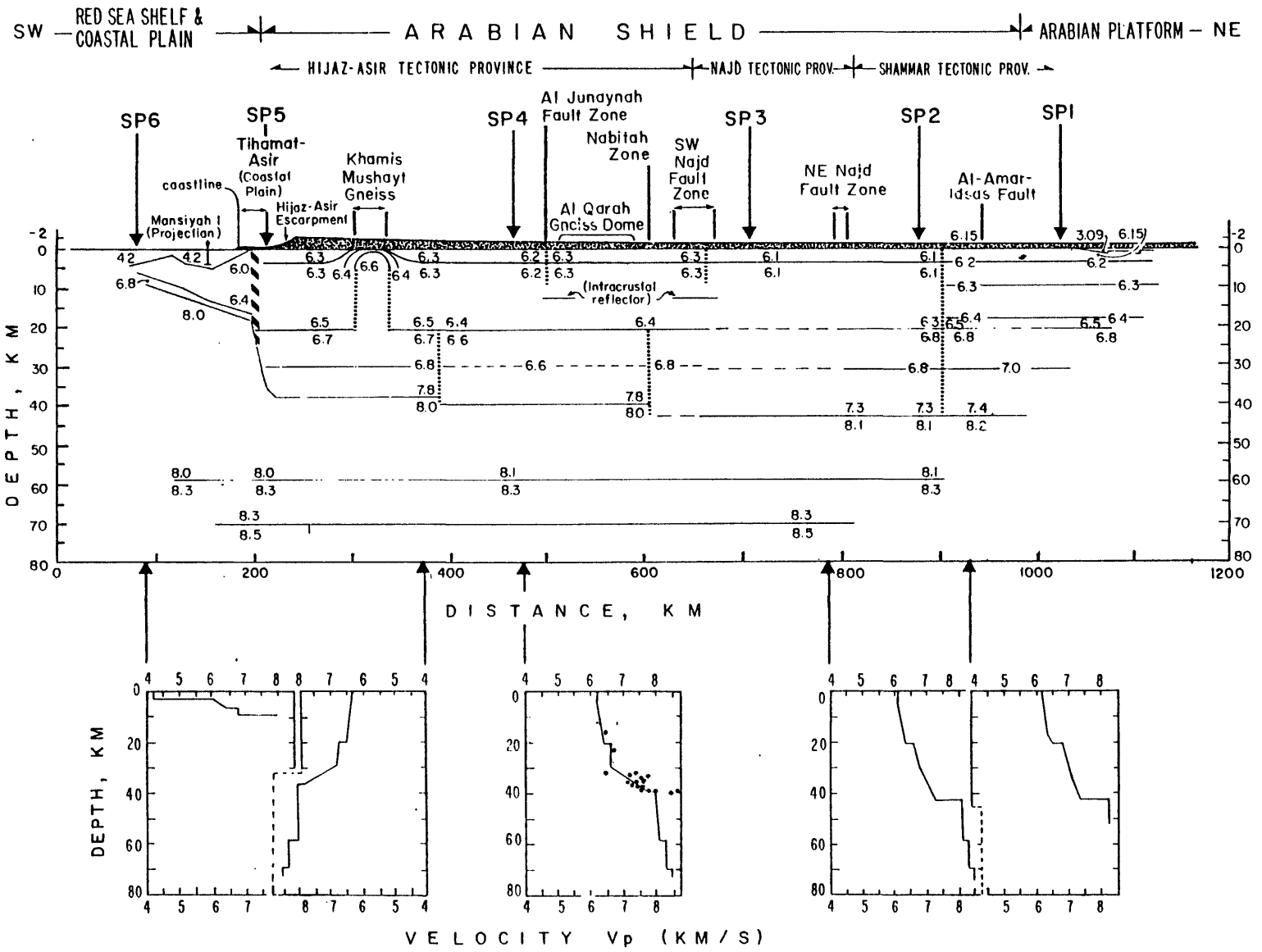

Figure 3.--Inferred crustal section for southwestern Saudi Arabia from the seismic deep-refraction data (adapted from Healy and others, 1982). Velocity-depth functions are shown in the lower part of the figure for the major tectonic provinces. Data points on velocity-depth function below SP4 are measurements from rocks of the Ivrea zone, northern Italy (Fountain, 1976).

model very similar to that of the Ivrea zone (Fountain, 1976).

For the Najd tectonic province between shot point 3 and shot point 2, the velocity-depth function fits the Ivrea model above the lower crustal layer, that is, above the granulite zone where velocities are slower than the Ivrea model. From the gravity profile analysis as well, we infer a lower mean density for the Najd tectonic province than for the Hijaz-Asir province, and conclude that at least the lower crust, and probably the entire crust, is less mafic in composition. At the surface in the Najd tectonic province, the layered rocks are dominantly andesitic volcanic and volcaniclastic, as opposed to basaltic southwest of the Nabitah zone.

The velocity-depth function northeast of shot point 2 shows reasonable agreement of velocities for the lower crust with the Ivrea data, but the intermediate crustal layer is significantly faster in velocity. Because we interpret this area to be an allochthonous continental block both on seismic and geologic evidence (Schmidt and others, 1978), we surmise that its crustal layers may well have different compositions. We interpret that the high velocity upper layer of the lower crust is caused by more mafic rocks in the amphibolite facies.

All of the velocity-depth functions for the Shield fall into the "Type II" category of Jones (1981). This classification of Precambrian lower crustal layers is divided into: "Type I-Normal" that have an average compressional wave velocity (V_p) of about 6.6 km/s and high electrical resistivity; "Type II-Intermediate" with a higher velocity (V_p 7.0 km/s or a gradient, 6.7 to 7.2 km/s) and moderate electrical resistivity; and "Type III-Low" in which there is a low velocity shear wave zone, V_p similar to Type II, and very low electrical resistivities. Type II crusts seem to surround Type I and were suggested as an evolutionary stage of a Shield by Jones (1981), who also suggested that Type I crust may never develop if a Shield does not have a certain minimum size. Jones observed that amphibolitic compositions meet the velocity and electrical resistivity requirements for the Type II crust and proposed that a Type II lower crust would have large proportion of hydrous minerals.

Our data are compatible with this interpretation although we have no electrical resistivity data to complement the seismic results. We know that the crustal velocities at the Mohorovicic discontinuity are significantly higher to the southwest of the Nabitah zone than those predicted by the model of Jones (1981). However, in light of the generalized nature of the Jones model and the agreement of the velocity-depth function with the data for the Ivrea zone (Fountain,

1976) we do not regard this difference in velocity to be an incompatibility with the model but instead a variation of it caused by differences in composition between the rocks of the two areas.

Bouguer gravity anomaly map

Gravity survey data collected at a station density of 1 per 100 km^2 is shown in figure 4 as a simple (no terrain corrections) Bouguer gravity anomaly map (Gettings, 1983). The most striking features of the map are the linear gravity high with positive Bouguer gravity anomaly values along the Thiamat-Asir and eastern edge of the Red Sea shelf and the steep gradient that is approximately centered on the outcrop edge of the Shield where the gravity anomaly field falls from positive to negative values of -100 mgal or more. The lithologic contact between Tertiary and Precambrian rocks occurs approximately at the halfway point on the gravity anomaly gradient, and because the gradient is approximately antisymmetric we infer that the contact dips steeply. To the northeast, the regional gravity anomaly pattern is broad and concave for about 400 km, with a minimum value of about -180 mgal. Northeast of the Nabitah suture zone (fig. 1), the regional gravity anomaly values begin to increase. The regional gradient is nearly linear and is approximately 0.13 mgal/km between the Nabitah suture zone and the edge of the Shield.

Gravity modeling of a profile taken between shot points along the transect (Gettings, 1977) indicates that the density of the crust southwest of the Precambrian Shield boundary is characteristic of oceanic crust. The model calculations also show that the regional gravity anomaly pattern, which is broad and concave from shot point 5 to the Nabitah zone, and linearly increasing northeast of the Nabitah zone, can be matched if the entire crust southwest of the Nabitah zone is of somewhat higher average density than that to the northeast. This higher mean crustal density is consistent with Schmidt and others (1978), who interpret the crust southwest of the Nabitah zone to be more mafic in composition.

Trends on the gravity anomaly map (fig. 5) fall into four distinct sets: east; north; northeast; and northwest. The ranges of each trend set are fairly narrowly defined, especially for the east and north sets. The north and east sets seem to be the oldest, as they are systematically interrupted or offset by the northeast and northwest trending sets. We interpret the northwest set to be associated with the late Precambrian Najd tectonic event because of their direction and their coincidence with mapped Najd faults. The northeast set of trends is presumably the signature of a conjugate set of fractures developed at the same time.

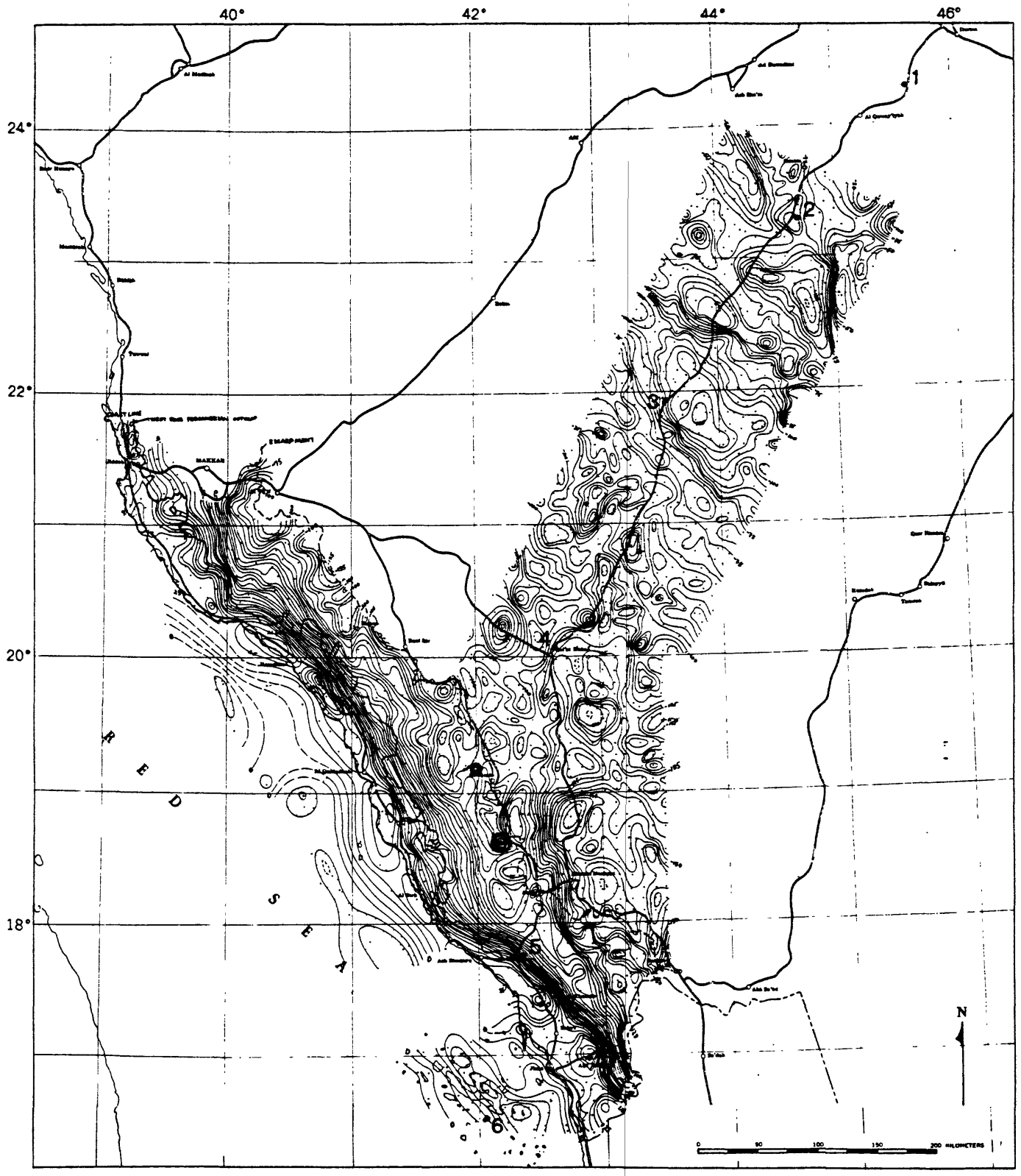

Figure 4.—Simple Bouguer gravity anomaly map of the geophysical transect and Asir escarpment-coastal plain area northwards to Jiddah. Contour interval is 5 mgal. The traces of the Red Sea coastline, outcrop edge of Precambrian rocks, and Asir escarpment summit are shown for reference. No terrain corrections have been applied. Steep gravity gradient along the edge of exposed Precambrian crust marks the transition from Arabian Shield continental crust to the northeast to Red Sea oceanic crust to the southwest. Locations of shot points 2 to 6 are shown for reference.

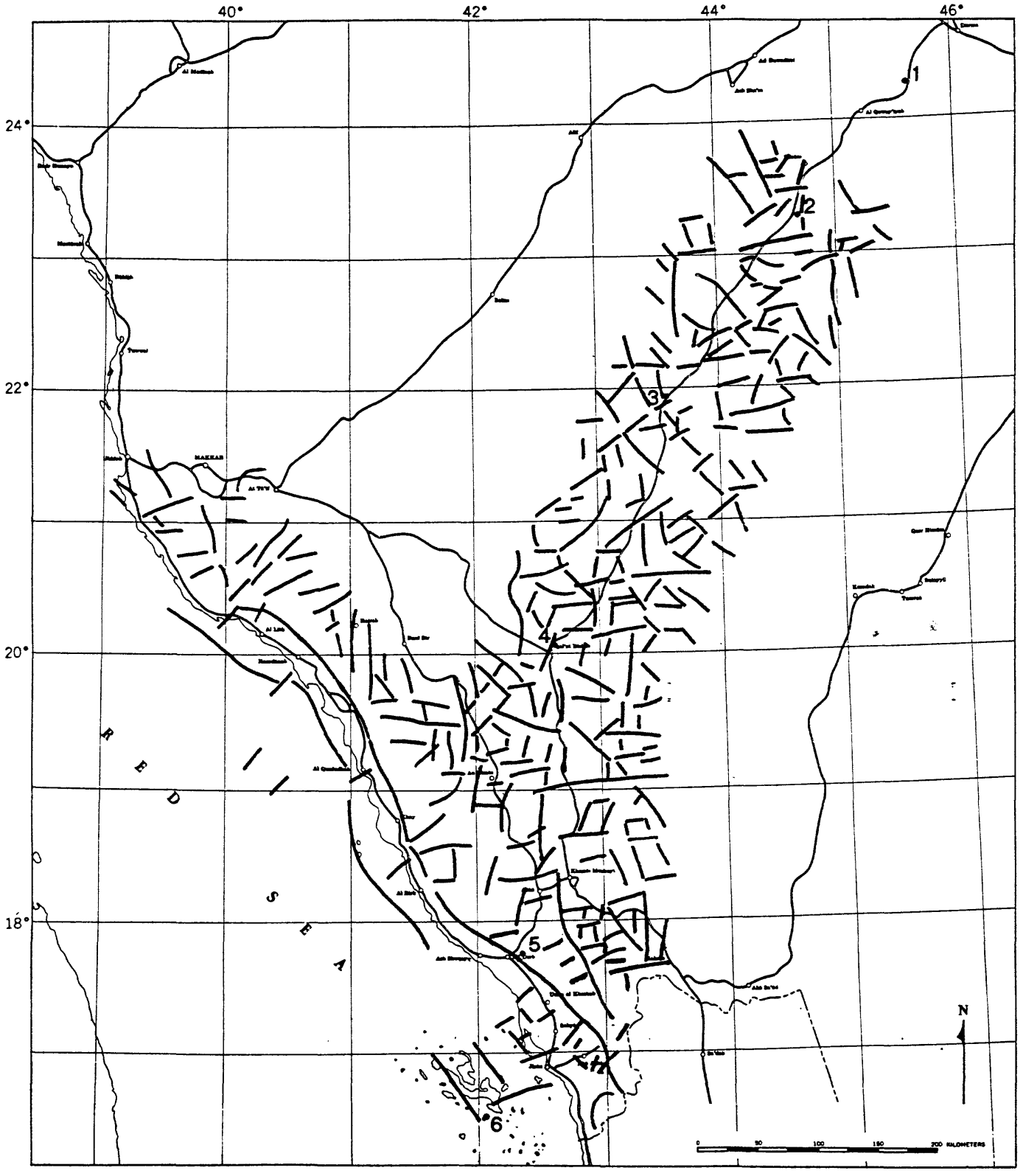

Figure 5.--Trend lines interpreted from the Bouguer gravity anomaly map.

The age relationship between the east and north trend sets is unclear. Both interrupt and sometimes apparently offset each other. The east set has the least expression in the mapped geology and thus may reflect deeper crustal structure. The outcrop patterns of the large batholithic complexes appear to be influenced by both sets and thus these trends may reflect deep seated, old fracture systems.

Superimposed on this pattern are many positive and negative local gravity anomalies of up to about ±30 mgal amplitude. The large troughlike negative anomaly at the southwest end of the transect is almost certainly due to salt diapirism beneath the emergent Farasan Islands. The three southernmost local positive anomalies within the linear positive gravity anomaly on the Tihamat-Asir are associated in part with outcropping Tertiary layered gabbro bodies. As can be seen by the trace of the escarpment in figure 4, terrain effects cause only local perturbations to the anomaly field, and although terrain corrections will smooth the map in the escarpment area, the gross features will remain unchanged.

The positive anomalies usually correlate with areas of greenstone, greenschist or diorite outcrop, and the negative anomalies correlate with areas of granitoid intrusives (figs. 2 and 4). Both the southern Najd fault zone and the northern Najd fault zone have positive gravity anomalies. These zones also show strong magnetic anomalies and have numerous mafic dikes along them (Jackson and others, 1963). We infer that the anomalous magnetic and gravity responses are caused by the mafic intrusives in the Najd fault zones.

The broad local positive gravity anomaly near the northeast end of the profile correlates with the high-grade metamorphic rocks that outcrop northeast of the Al Amar-Idsas thrust fault.

Aeromagnetic map

The regional features of the magnetic field are shown on the map in figure 6 which is generalized from the aeromagnetic map of the Shield (Andreasen and others, 1980). The aeromagnetic data were collected at 150 m mean terrain clearance except near the southwest end, starting midway between shot points 4 and 5, which was completed at 300 m clearance due to the rugged topography.

At the northeast end of the transect the block to the east of the Al Amar-Idsas thrust fault is characterized by large-amplitude, short-wavelength anomalies (10 km or less) that correlate well with the high-grade metamorphic rocks and intrusives that crop out there. Across the thrust fault, the magnetic field changes radically, becoming very flat and of low intensity; this pattern extends nearly to the northeast

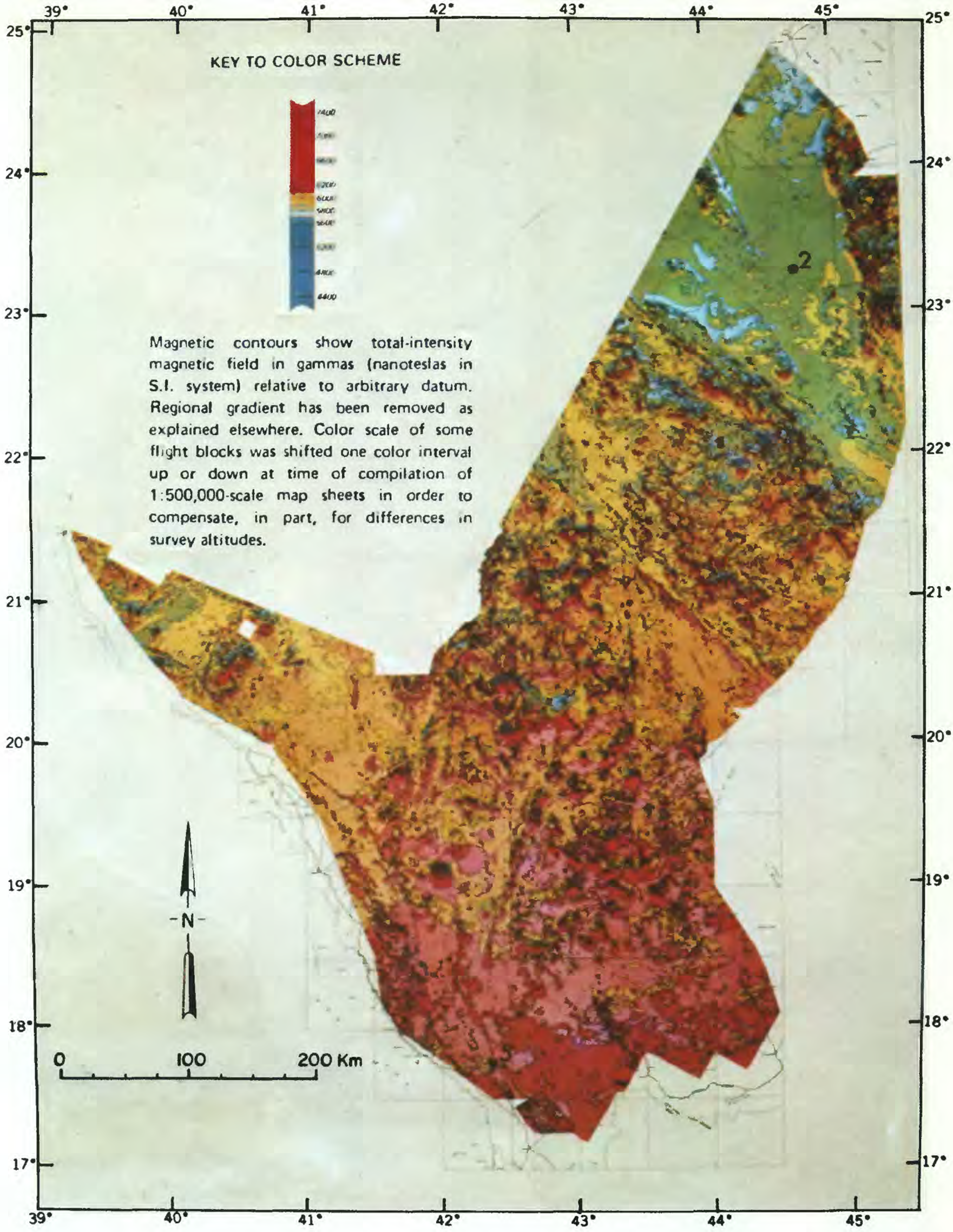

Figure 6.--Photograph of a part of the total-intensity aeromagnetic map of the Arabian Shield showing the geophysical transect area. The contour interval is variable. Shot points 2 and 5 shown for reference. (From Andreasen and others, 1980).

Najd fault zone, although some expression of the Uyaijah ring complex (Dodge and Helaby, 1979) is seen just northeast of the Najd fault zone. This large magnetic quiet zone is similar to those found over stable granitic blocks of crust in both the Canadian and Australian Shields.

The Najd tectonic province (fig. 1) is characterized by numerous, short-wavelength (~ 5 km) magnetic anomalies, many of which may be due to east and northwest trending mafic dikes. These anomalies are, in general, not as intense in amplitude as those of the crustal block east of the Al Amar-Idsas thrust fault. In addition, longer-wavelength (~ 10 km), variable-amplitude anomalies are superimposed on the pattern. The short-wavelength anomalies continue across the southern boundary of the Najd province, although not in such profusion. Whether this pattern persists to the southwest more than halfway between shot points 4 and 5 is uncertain because of the change in mean terrain clearance to 300 m.

Trends in the aeromagnetic map (fig. 7) fall into the same four groups as in the gravity anomaly map (fig. 5) and generally correlate well with them although many more trend lines can be defined on the aeromagnetic map because of the much higher data density and consequent increase in detail of the map. As on the gravity map, northeast and northwest trend sets on the aeromagnetic map appear to be the youngest and north and east sets seem to be the oldest. In addition, curvilinear trends appear in the southern half of the aeromagnetic map (fig. 7) which define roughly circular zones 50-100 km in diameter and generally correlate with the large granitic bathololithic complexes. These circular trend features identify batholithic-size zones of repeated granitic intrusive activity in the upper crust which have lowered the average bulk magnetization of the zone. These areas thus appear as a circular zone on the aeromagnetic map with a magnetic response which is on the average low, and are termed magnetic "quiet zones".

The southward increase in overall magnetic intensity observed is partly a relic of the data reduction because the regional variation was removed arbitrarily from the flight path profiles when the contractor compiled the maps (Andreasen and others, 1980). Therefore, this trend probably does not reflect an actual overall southward increase in magnetization of the crustal rocks.

The magnetic signatures of the block east of the Al Amar-Idsas zone (figs. 1 and 7) are distinctive, especially in map view (Andreasen and others, 1980), and suggest that this block represents a crustal type different from the rest of the Shield, in agreement with Schmidt and others (1978) and Stacey and others (1981).

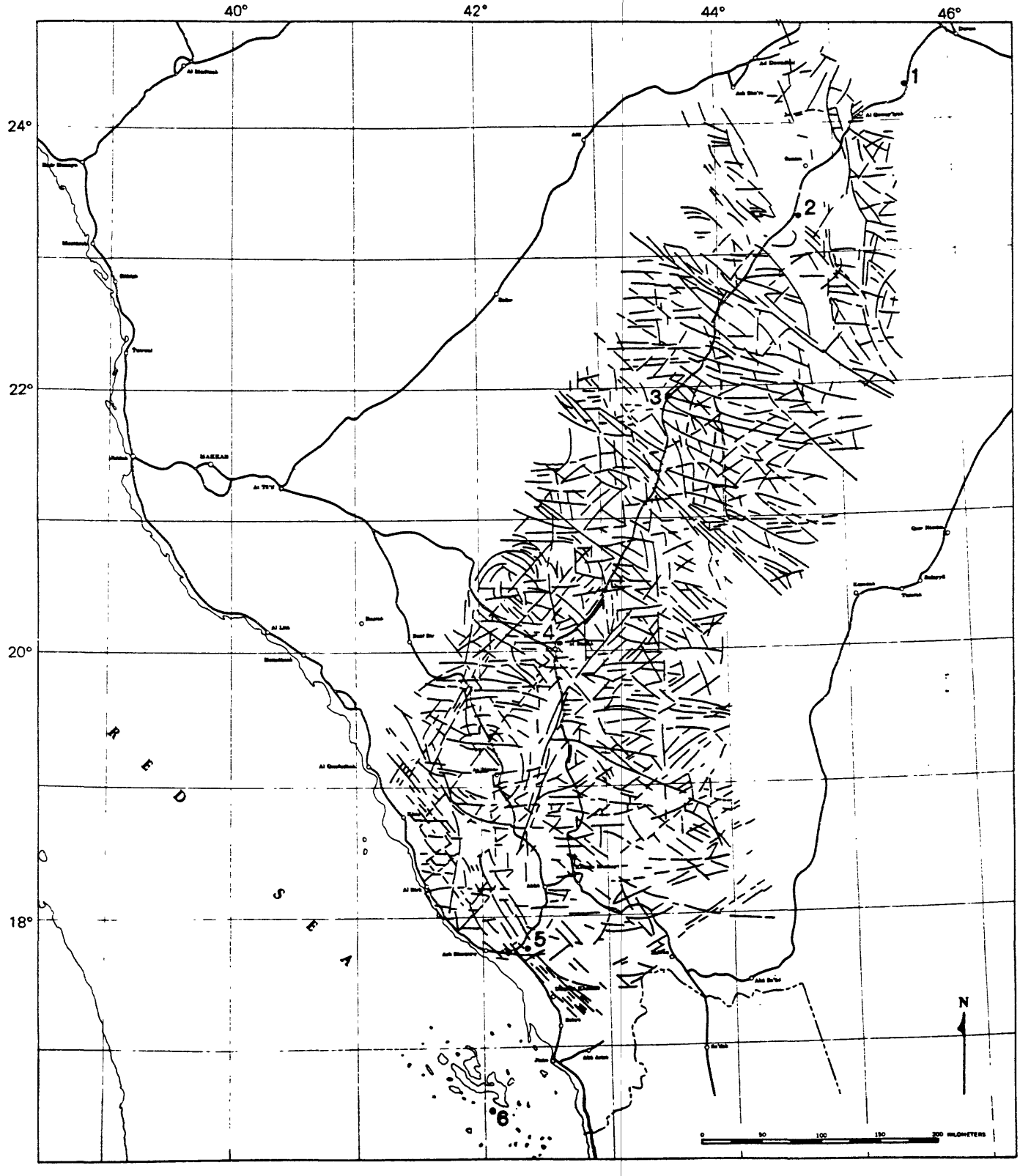

Figure 7.--Trend lines interpreted from the aeromagnetic map.

Heat flow profile

The heat flow measurements made during the seismic refraction field work in 1978 were the first to be made on the Arabian Shield. They were completed at shot points 1 through 5 by temperature-logging of the drill holes before the explosives were loaded. We determined thermal conductivities by modal analyses of thin sections of core and surface samples taken at the shot points. At shot points 2, 3, and 4, drill holes were in granitic rocks, and heat production was measured. The plot of heat production versus heat flow is strongly nonlinear; however, as there were only three measurement locations, more data are needed to confirm the nonlinear relationship.

We have included heat flow values from the deep petroleum exploration drill hole Mansiyah 1 (Girdler, 1970), and from the Red Sea shelf and axial trough (Girdler and Evans, 1977) in the heat flow profile shown in fig. 8. We refer the reader to the results of a detailed analysis of the 1978 heat flow data given in Gettings (1981; 1982) and Gettings and Showail (1982).

The profile (fig. 8) shows an increase in heat flow toward the Red Sea margin. Assuming an exponential heat source distribution (Lachenbruch, 1970), extrapolation of geotherms yields a temperature at the base of the crust beneath shot point 4 that, even considering uncertainties, is higher than that below shot points 2 or 3.

The high heat flow at shot point 5 can be explained by heating from the abutting oceanic crust and(or) an enhanced mantle component of heat flow through the thin continental crust, provided the higher temperature regime has persisted for 10 Ma or so (Gettings, 1982). In order to maintain the high heat flow values observed on the Red Sea shelves and coastal plains (Girdler and Evans, 1977), a model with a mass flux of hot material at the base of the lithosphere seems necessary if the age of this crust exceeds about 5 Ma (Gettings, 1982). Finally, in the actively spreading axial trough, classical sea-floor spreading models that allow for hydrothermal convective activity are adequate to explain the observed heat flow (Gettings, 1982).

Previous seismic work

Girdler (1969) reviewed early seismic work in the Red Sea. The pioneering surveys made in 1958, using two ships, included 15 refraction profiles in the northern, central, and southern sectors (Drake and Girdler, 1964). Profiles in the southern sector show a sedimentary cover 0.5-4.5 km thick (velocity 3.49-4.48 km/s) that consists largely of the Miocene evaporite and clastic deposits. For deeper layers,

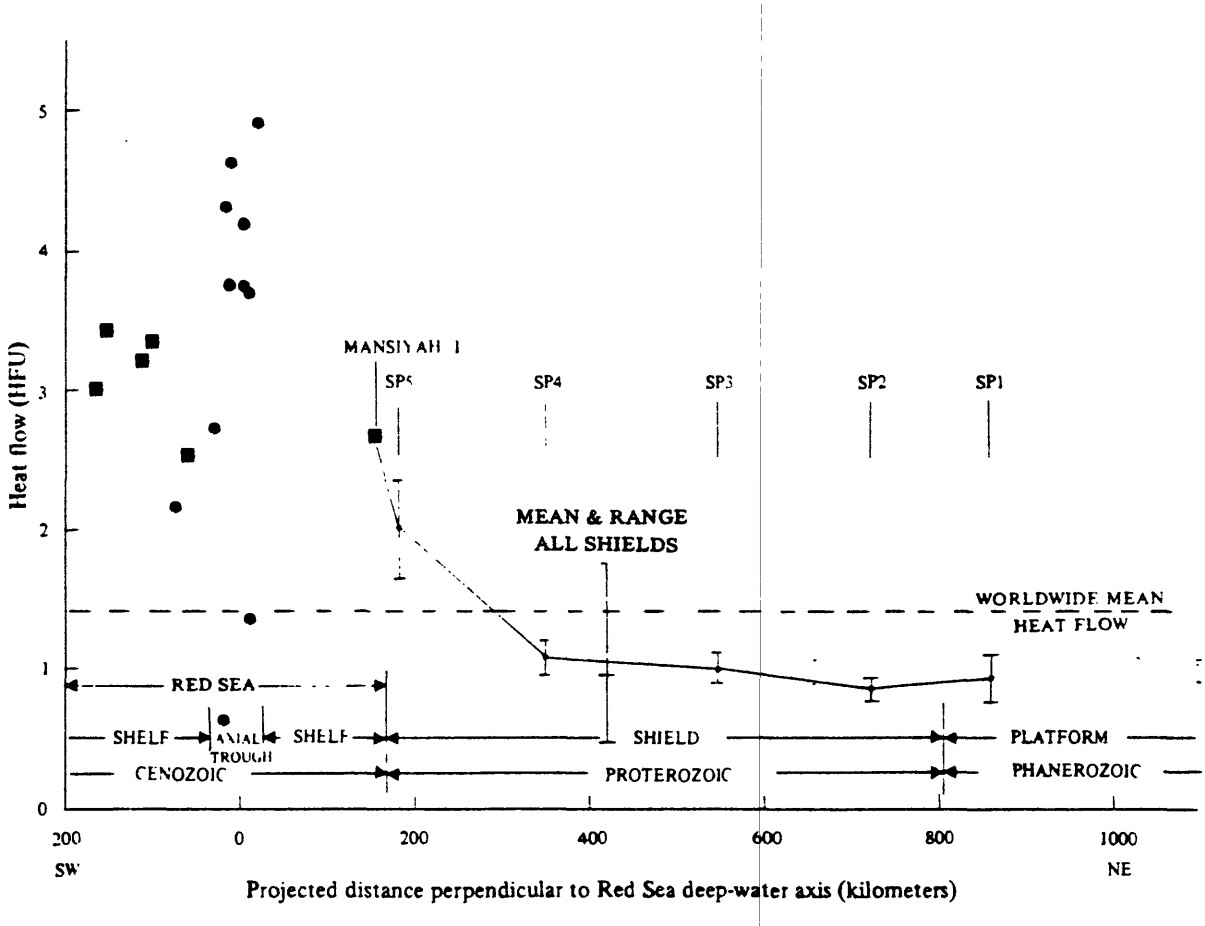

Figure 8.--Plot of heat flow as a function of distance from the Red Sea deep-water axis shown on figure 2. Heat flow data other than SP1-SP5 are from Girdler and Evans (1977). One HFU is 1 E-6 cal/cm^2/s or 0.04187/Wm^2. For points in the Red Sea, solid squares are on the shelf, solid circles are in water deeper than 1 km.

similar results were obtained in all three sectors of the Red Sea; velocities over the axial trough were mostly in the range 6.8-7.3 km/s, and velocities over the main trough were mostly in the range 5.8-6.1 km/s. Girdler (1969) interpreted the high-velocity basement in the axial trough as oceanic crust and the lower-velocity basement on the shelves as continental material. For oceanic basins, the arithmetic mean seismic compressional wave velocity of layer two, the upper layer of oceanic crust, is only about 5.1 km/s (Hill, 1957; Raitt 1963; Le Pichon and others, 1973), with a standard deviation of 0.6 km/s; if velocities for oceanic crust of Tertiary age are not greatly different from the arithmetic mean figures, then the lower-velocity basement reported by Girdler (1969) could be oceanic or continental.

Other seismic work in the Red Sea includes continuous ("sparker") reflection profiles over the main and axial troughs (Knott and others, 1966; Phillips and Ross, 1970), and refraction profiles on the shelf of the northern and central sectors (Tramontini and Davies, 1969). The central sector survey, which covered a limited area in detail found an average basement velocity of 6.6 km/s and an average basement depth of 4.6 km for the portion of the main trough adjacent to the axial trough.

The seismic refraction data available clearly indicate that material with oceanic crustal velocities is present in the axial trough and that the basement of the main trough is composed, at least in part, of oceanic crust. Whether continental crust also underlies the thick sediments on the shelves is controversial. Very little information has been obtained on velocities or crustal thicknesses beneath the landward portion of the shelves, due chiefly to the difficulty of navigation in the shallow reef zones.

The seaward portion of the coastal plain in southwest Saudi Arabia was studied by seismic reflection methods (Gillmann, 1968). The surface of basement dips toward the Red Sea at an average angle of about 10 degrees; its depth increases from about 2 km some 20 km inland to nearly 5 km in the vicinity of the Mansiyah 1 drillhole and Jizan salt dome (the coastline). Unfortunately, the Mansiyah drillhole had to be discontinued just short of where it would have intersected the seismic basement. The profiles did not extend onto the Precambrian Shield, and the nature of the basement remains speculative.

No seismic deep-refraction data have previously been obtained for southwestern Saudi Arabia. Studies of shear waves on the path Addis Ababa, Ethiopia-Shiraz, Iran (which passes through the Afar depression in Ethiopia) have shown that the average crustal thickness for this region is about 35 km (Niazi, 1968; Knopoff and Fouda, 1975). Shear-wave

velocity models from these studies show a pronounced low-velocity zone with the top of the zone at 100-140 km depth (Knopoff and Fouda, 1975). Phase velocities of the Arabian Shield are lower than those of the Canadian Shield; however, they are higher than those of the United States Gulf Coastal Plain (Knopoff and Fouda, 1975).

FIRST ORDER STRUCTURE OF THE ARABIAN SHIELD AND ITS MARGINS

General remarks

To a first-order approximation, the Precambrian Shield (fig. 3) is composed of two layers. The upper crust is 21 km thick with an average velocity of about 6.3 km/s; a first-order velocity discontinuity at which velocities increase from about 6.4 to 6.7 km/s marks its base. The lower crust is about 19 km thick with an average velocity of approximately 7.0 km/s; a velocity increase from 7.3-7.9 km/s to 8.0-8.2 km/s marks the base of the crust (Mohorovicic discontinuity). The depth to the M-discontinuity generally decreases toward the Red Sea, from 43 km in the northeast to 38 km in the southwest. Across the ocean-continent transition at the western margin of the Shield, the crust thins abruptly, to less than 20 km. Beneath the sedimentary section of the Thihamat-Asir coastal plain and Red Sea shelf, the average crustal velocity is 6.2 km/s.

Although this first-order model fits the average travel times of the record sections, significant deviations from predicted arrival times and varying frequency content and amplitude of individual seismograms indicate lateral inhomogeneities within the crust. Detailed comparison of the geologic sections with the record sections shows considerable correlation between velocity variations and lithologic and structural features.

Western Shield margin and the Red Sea rift and shelf

The most dramatic crustal and upper mantle structural change along the profile is the transition from the westernmost Shield to the Red Sea rift and shelf. The Shield directly beneath shot point 5 (fig. 3) appears to have roughly the same velocity structure as the average throughout the Shield. The transition to the thin crust of the shelf occurs over the short distance of 20 km southwest from shot point 5. The seismically-determined transition is characterized at the surface of the Tihamat-Asir by a sharp boundary between the Precambrian rocks and the Tertiary volcanic and intrusive rocks (fig. 3).

A simple three-layer crust of sediments (V_p=4.2 km/s), upper crust (V_p=6.2 km/s), and a thin lower crust (V_p =6.8 km/s) characterizes the Red Sea shelf and the coastal

plain. The crust thins from 17.5 km at the coast to 8 km at shot point 6, and the mantle velocity is 8.0 km/s.

Any seismic crustal model is subject to constraints imposed by the gravity and magnetic data. The Bouguer gravity anomaly map for the coastal region shows the steepest gradient centered over the exposed margin of the Arabian Shield, about 65 km west of the Hijaz-Asir escarpment. This gradient connects the highly negative (-100 to -140 mgal) gravity anomaly field of the Shield interior to the gravity field of the coastal plain and Red Sea shelf, where values are close to zero. The steepness of the gradient is accentuated by the hypabyssal gabbroic intrusive bodies in the marginal zone.

The mean velocity of the seismic basement beneath the coastal plain and Red Sea shelf in this region, 6.2 km/s, falls well within the range for diabase, 6.1-6.7 km/s (Nafe and Drake, 1968). Therefore, we interpret the basement as consisting largely of diabase of a sheeted dike complex. This conclusion agrees reasonably well with the gravity data. Gettings (1977), assuming isostatic equilibrium and taking into account the known thickness of low-density sedimentary rocks, has shown that the gravity level change is compatible with a density contrast between oceanic and continental crust but not with that of an intracontinental crustal boundary.

Aeromagnetic data onshore and offshore in the vicinity of the seismic profile support the hypothesis of a diabase basement beneath the shelves and coastal plain. Girdler and Styles (1975), Hall and others (1976), and Hall (1980) mapped large-amplitude, long-wavelength linear magnetic anomalies along the shelves of the southern Red Sea and interpreted them as the expression of oceanic crustal strips of alternating remanent polarization that were emplaced during Tertiary sea-floor spreading, and subsequently buried by Miocene sedimentary deposits. These anomalies extend onto the coastal plain and inland as far as the exposed margin of the Shield, where they are associated by Blank and others (1981) and Kellogg and Blank (1982) with the diabase dike swarm in the structural transition zone.

In this seismic interpretation we have presented a continental crust of "normal" thickness and velocity structure beneath the Arabian Shield, a crust of "transitional" thickness and velocity structure near the Shield margin, and a crust of "normal" oceanic thickness and "transitional" velocity beneath the Red Sea shelf. The crust near the Shield margin (shot point 5) is probably about 16±4 km thick; it probably consists chiefly of diabase, because such a crust would satisfy the constraints imposed by the seismic refraction, gravity and aeromagnetic data, and diabase is the chief component where basement is exposed. The observed velocity of 6.2 km/s is intermediate between the velocities of typical

oceanic Layers 2 and 3 of ocean basins, but the seismic data alone do not discriminate between diabase, a mixture of Layers 2 and 3, and a typical sialic crust. This crust passes westward into crust of "normal" oceanic thickness of about 4 km underlying the Miocene sediments of the outer Red Sea shelf.

Modeling of the Bouguer gravity anomaly profile

A generalized version of the refraction section together with a profile of the simple Bouguer gravity anomaly field taken from the gravity map (fig. 4) along straight line segments between the shot points is shown in figure 9. This section retains the major features of figure 3 and was used to define the geometry for model calculations of the gravity profile. The average velocities shown on figure 9 were calculated from total travel times for a vertical ray through the layer with the velocity distributions of figure 3. Starting density values for the model were obtained from the average velocity data by using experimental velocity-density relations (Nafe and Drake, 1968) and considering the likely gross lithologic composition of the block derived mainly from Schmidt and others (1978). Because of the good correlation between the velocity-depth functions between 230 and 600 km on fig. 3, and the measured velocity data for the Ivrea zone (Fountain, 1976), the Ivrea zone velocity-density data was given extra weight. Even so, the assigned density to a block for a given velocity is uncertain by about ± 0.12 gm/ cm^3 so that we are free to adjust densities within this range to fit the observed gravity field and still have a valid model constrained by both the gravity and seismic refraction data.

Gravity models were calculated with a computer program by using a standard two-dimensional polygonal model formulation (Talwani and others, 1959) and the resulting best density model after about 20 adjustments is shown on figure 9. Since the density contrast is the actual parameter in this work, all density values on figure 9 can be increased or decreased by a constant amount if desired. The gravity model calculations are compared with the observed profile data in figure 10. In order to fit the northeastward-trending regional increase in the gravity field, and keep the density values of the section reasonable, it was necessary to add a component from the deep upper mantle (59-115 km depth) with density contrast increasing to the northeast. This was accomplished by computing the effect (fig. 10) of a rectangular prism with a linearly increasing density contrast to the northwest from the 400 km point on the profile (fig. 9) to the 1000 km point. A total density contrast of 0.05 gm /cm^3 across this distance was used. In order to eliminate edge effects, both this prism and the crustal model of figure 9 were extended to the northeast to 10,000 km and the entire model

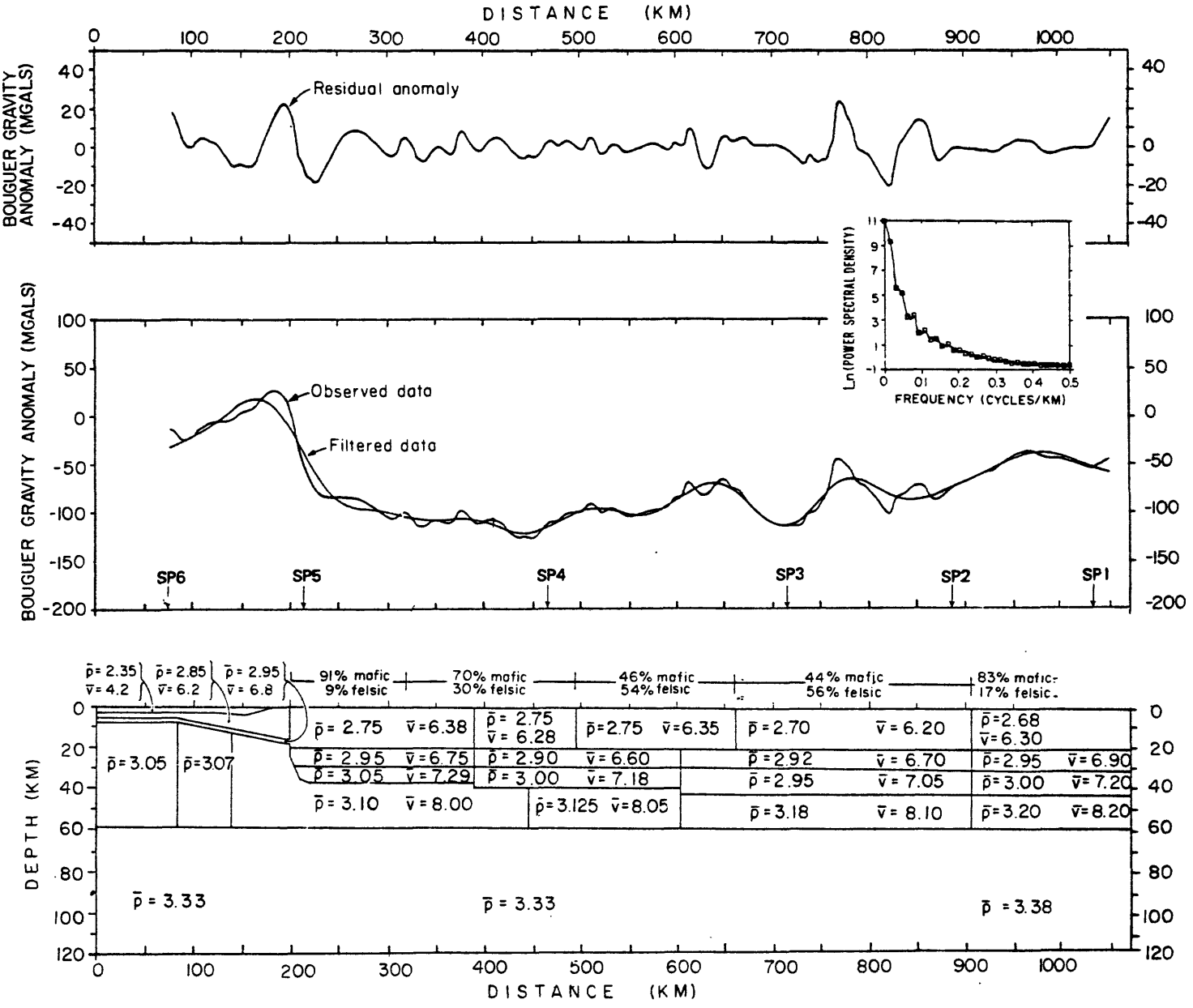

Figure 9.--Generalized crustal section for southwestern Saudi Arabia showing the bulk mean velocity (v) and density ($\bar{\rho}$) values adopted from analysis of seismic refraction and gravity anomaly data. Bouguer gravity anomaly data from a profile taken along straight line segments between shot points, a low-pass Fourier filter (50 km half-wavelength cutoff frequency), and resulting residual gravity anomaly profile are shown. Power spectral density estimates of the gravity anomaly profile are shown in the inset. The fit of the model to gravity data is shown in figure 10. The mafic and felsic percentages for the geologic provinces on the Shield are computed from the trace of the profile on the 1:2,000,000 scale geologic map (U.S. Geological Survey-Arabian American Oil Company, 1963).

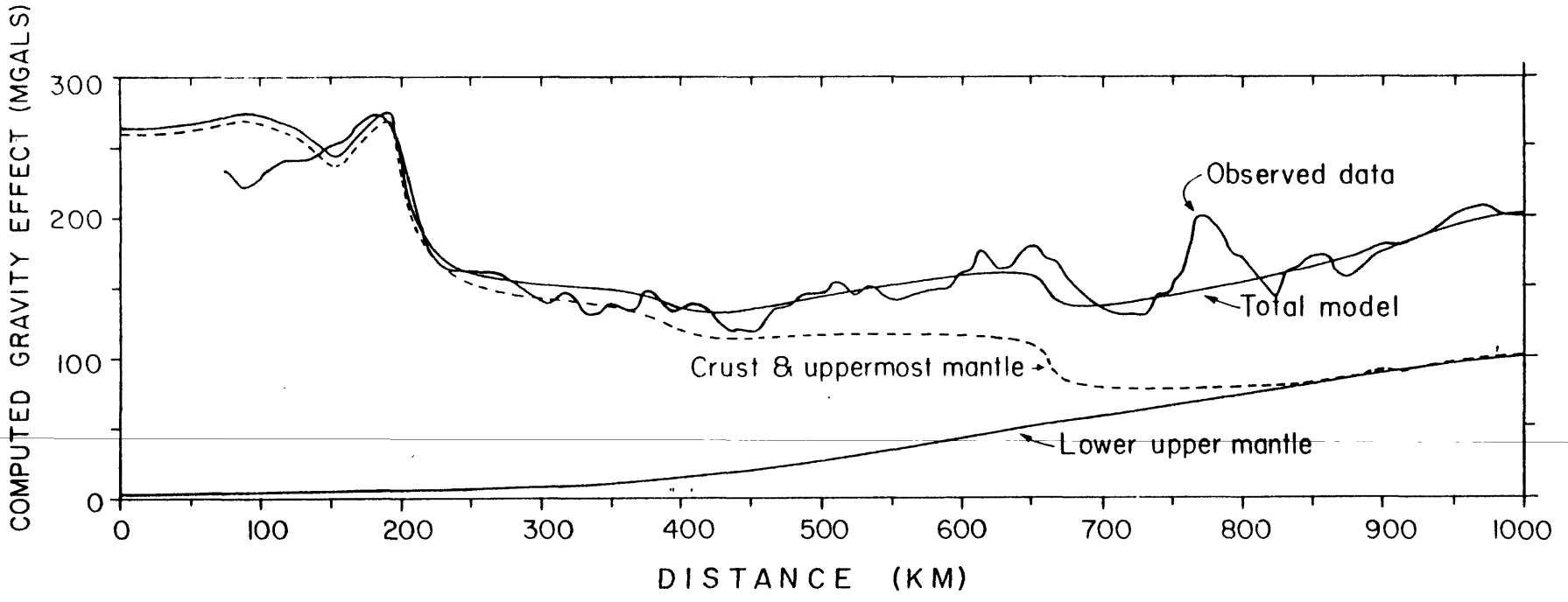

Figure 10.--Gravity effect of the section of figure 9 compared to the observed data profile. The dashed line shows the computed effect of the section above 59 km depth; the lower solid line shows the effect of the "lower" (59-115 km) part of the upper mantle. The discrepancy at distances less than 150 km is due to the effects of the water in the Red Sea and variations in evaporite thickness in the Miocene sedimentary sequence which were not computed.

was reflected about the origin. The resulting model fits the gravity profile, if the local anomalies attributable to upper crustal sources which generally correlate with the surface geology are ignored. The discrepancy at the origin of the model can be accounted for by including the gravity effect of the average water depths in this part of the Red Sea; this was not included in this model because detailed gravity data were not available to extend the profile. We interpret the northeastward increase in density contrast in the mantle to reflect the thermal regime in the mantle due to the sea-floor spreading system of the Red Sea; that is, hot, less dense aesthenosphere material upwelling along the Red Sea axis and flowing and cooling laterally beneath the lithosphere of the Arabian Plate. Analysis of the available heat flow data support this hypthesis (Gettings, 1982). The pronounced low velocity zone in the deep upper mantle (Knopoff and Fouda, 1975) also supports the convective flow model. The densified lowermost crust between 200 and 400 km (fig. 9) along the profile we infer to be the result of intrusive activity which must have accompanied the continental rifting process.

Upper mantle velocities at the M-discontinuity vary from 8.0 km/s between shot points 6 and 3 to 8.1-8.2 km/s between shot points 3 and 1. The velocity-depth function of the upper mantle is unexpectedly uniform along the length of the profile; there is a first order discontinuity at 60 km with a velocity increase from 8.0 or 8.1 to 8.3 km/s and another 10 km deeper, from 8.3 to 8.5 km/s. The M-discontinuity seems to be sharp, occurring across a zone of narrow width along the entire profile. In the Arabian Shield southwest of the Nabitah zone (between shot points 3 and 4), there is a constant 0.2 km/s increase at the M-discontinuity, although absolute velocity values of the crust and mantle decrease to the southwest. The M-discontinuity is also sharp beneath the Red Sea shelf, with a velocity contrast of about 1.2 km/s over a very narrow zone.

The thickness of the crust, defined by the depth of the M-discontinuity, increases eastward in our model, varying from ~8 km near the Red Sea axis to 18 km beneath the shelf and coastal plain, increasing abruptly beneath the western margin of the Shield to 38 km, and increasing gradually to 43 km beneath the allochthonous continental block near shot point 1. Most of the interpretations by participants in the Commission for Controlled Source Seismology Workshop, Park City, Utah, 1980 (Healy and others, 1982) show roughly the same relationships, except that several have a zone of thickened crust (to about 42 km) in the area of shot point 4 and westward.

None of the interpretations of the seismic refraction data to date show the thickest crust coincident with the area of greatest topographic relief; models that feature a thickened crust between shot points 5 and 4 all show the thickest crust displaced by varying degrees (up to 200 km) to the east of the topographic maximum. This observation implies a less dense upper mantle towards the west, at least from shot point 4 onward, if isostatic equilibrium is to be maintained. The more mafic character of the crust from the Nabitah suture zone westward (Schmidt and others, 1978) offsets the need for a less dense upper mantle somewhat, but not entirely. The seismic observations are in agreement with the peculiar shape of the regional gravity profile described above. The gravity relations, as constrained by isostasy, seismic refraction, and geologic considerations, require both a more dense crust west of the Nabitah zone and a less dense upper mantle. These observations are in agreement with intuitive models of an upper mantle convective system that one might expect to be associated with the Red Sea spreading system. Assuming that the minimum mantle flow rates comparable with the Red Sea floor spreading rates have been operating throughout the Tertiary, the lower lithosphere beneath the profile would have been heated by convective flow in the aesthenosphere and isostatic processes would produce the regional uplift and regional gravity anomaly pattern we now observe.

In a second interpretation of the Bouguer gravity anomaly profile, we applied a low pass filter to the profile digitized at 1 km intervals to separate upper crustal from lower crustal sources. In figure 9, a filtered profile with a cut-off half-wavelength of 50 km and its residual are shown. The filtering was accomplished in the frequency domain using a modified Hamming window after linear detrending of the profile and subtraction of the mean value. Filtering the profile at half-wavelength of 5 and 10 km yielded a result identical to the data profile, a reassuring result since the gravity data were collected at an average spacing of 10 km. For a compact source, a half wavelength of 50 km yields a depth of 15 km or greater; therefore, the filtered profile represents mainly lower crustal and deeper sources.

The estimates of power spectral density (inset, fig. 9) suggest that the low frequency part of the spectrum is composed of two overlapping peaks, one at frequencies up to about 0.025 cycle/km and another from 0.025 to about 0.05 cycle/km, corresponding to sources below approximately 10 km and above about 5 km, respectively. A filter corresponding to about 10 km and deeper depths (30 km half-wavelength) was computed, but the residual gravity profile yielded very low-amplitude anomalies which did not correlate well with the surface positions of geologic contacts. The residual from the 50 km half-wavelength filter yields a good correlation with the surface geology and has reasonable

anomaly amplitudes, and we accept it as the best estimate of separation of deep from shallow sources of the gravity anomalies. Although distributed density changes in the upper crust would give longer wavelength components to the spectrum of the gravity field as well as deeper sources, we have no reason to suspect them from observations based on geologic mapping. Thus, we regard the upper crust as being composed of distinct lithologic units with sharp boundaries and attribute the longer wavelength components of the anomalous gravity field to mass variations at depth.

The low pass filtered profile (fig. 9) is in good agreement with the pattern of the gravity model of figure 10, so long as it is remembered that the model of figure 10 contains upper crustal sources as well. In particular, agreement is good for the the broad gravity minimum at 275-575 km on the profile and the northeasterly increasing gravity gradient beyond 575 km. We have ignored the initial and final 70 km of the filtered profile as subject to possible aliasing from the filtering process. Two large symmetric gravity anomalies appear at about 650 and 775 km and correspond to the linear gravity highs on figure 4 associated with the two Najd fault zones along the transect. Interpretation of these anomalies as infinite horizontal cylinders yields a depth to center-of-mass of about 36 km and a radius for a density contrast of 0.1 gm cm^{-3} of 18 km. The same procedure applied to the data profile (fig. 9) for the anomaly at 775 km yielded a depth to center-of-mass of 23 km and radius for 0.1 gm cm^{-3} density contrast of 12 km for the broad part of the anomaly. The narrow peak on the anomaly yields a depth of 9 km and radius for 0.1 gm cm^{-3} density contrast of 7.5 km for both the peak on the residual curve and the same peak defined by inspection from the data profile (fig. 9).

We interpret the anomalies at 650 and 775 km to be zones of mafic intrusive activity into both the lower and upper crust. The intrusive zones probably increase in size with depth below about 13 km, the level of the intracrustal seismic reflector (fig. 3) which we interpret as marking the top of the major intrusive zone. In the case of the northeastern gravity anomaly (fig. 4; 775 km on the gravity profile of fig. 9) a mafic dike swarm that trends parallel to the gravity high and beneath its axis (Jackson and others, 1963) may represent the uppermost expression of the intrusive events. No similar set of dikes is mapped on the southern anomaly (650 km on the profile of fig. 9). Because these anomalies correspond to the major Najd strike-slip fault zones, we infer that these fracture systems provided the crustal conduits for the postulated intrusive activity.

The velocity discontinuities in the upper crust, which cluster at 13 km depth (fig. 3) may indicate to an increase in crustal rigidity resulting in intrusive activity above

this depth. The inferred ages (post-Najd faulting) of these events are consistent with the final thermal pulse of the Pan-African event (Schmidt and others, 1978). Also, the 13 km depth is the same as the maximum depth of earthquakes along the San Andreas fault of central California (Eaton and others, 1970). If we postulate that the crustal heat flow in Saudi Arabia during the Pan-African event was comparable to the present-day heat flow in California (2 HFU), the seismic refraction interpretation is compataible with a generalized crustal model consisting of a brittle upper crust overlying a more ductile lower crust.

The broad gravity anomaly on the filtered profile (fig. 9) at 500 km is probably due to the presence of high-grade metamorphic gneisses of the Al Qarah gneiss dome (Schmidt and others, 1978).

Modeling of the aeromagnetic profile

An aeromagnetic profile was plotted along straight line segments between shot points from the 1:500,000-scale aeromagnetic maps (Andreasen and Petty, 1973, 1974a, 1974b). The profile was digitized at 1 km intervals and filtered as described for the gravity profile above. As interest was centered on defining the deep magnetic sources, we considered only the 50 km half-wavelength lowpass filtered profile (fig. 11).

The estimates of power spectral density for this profile (inset, fig. 11) show significant power at frequencies less than 0.1 cycle/km and a distinct peak between 0.1 and 0.2 cycle/km. This peak corresponds to a source shallower than about 5 km and probably represents the contribution to the spectrum of exposed or shallow plutons which are generally 5 km or less in thickness. The broad smooth shape of the spectral peak below 0.1 cycle/km is interpreted to indicate that there are sources throughout the crust for the profile as a whole.

The aeromagnetic map (fig. 6) contains broad smooth anomalies particularly associated with the east trend set and apparently coming from deep sources. In order to test this hypothesis, we interpreted the anomalies appearing on the filtered profile (fig. 11) by elementary methods to estimate the depth and horizontal extent of the causative sources. The horizontal extent of the steepest gradient was used as an estimator of depth and the position of maxima and minima was used to infer the horizontal extent. For a magnetic north-south profile at this magnetic latitude and an assumed magnetization in the direction of the earth's field, the appropriate prismatic models (Andreasen and Zietz, 1969) show that the edges of the body along the profile are near the maximum and minimum of the anomaly. The results are shown on figure

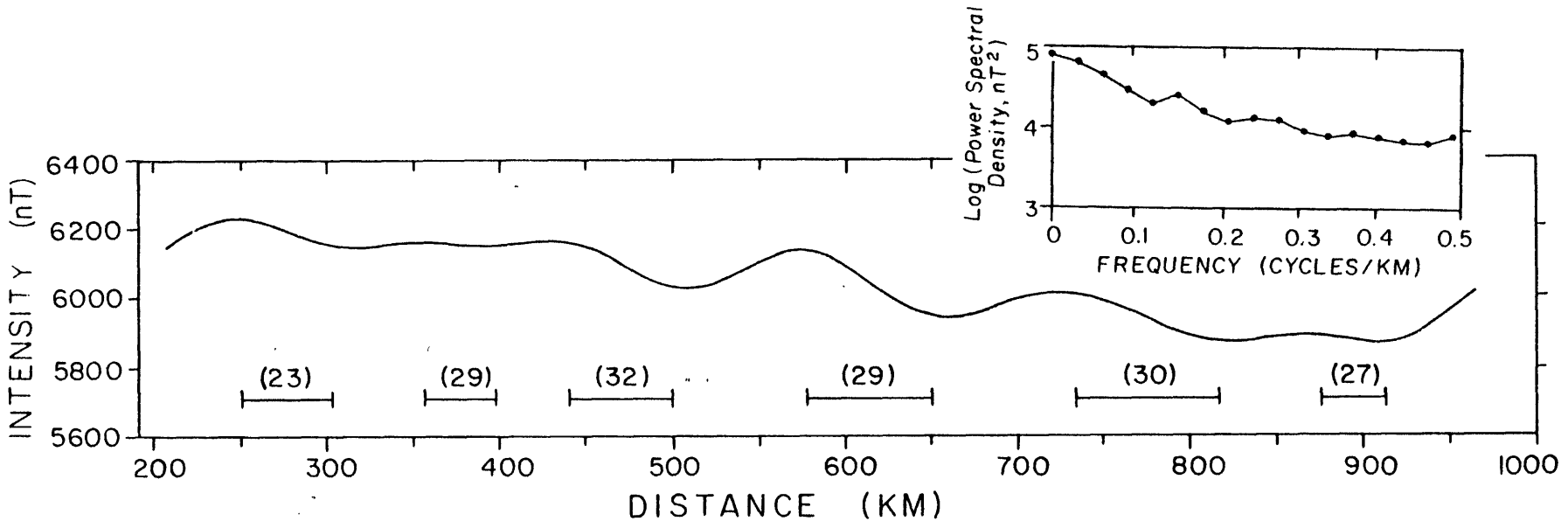

Figure 11.--Low-pass filtered aeromagnetic data from aeromagnetic map taken along a profile defined by straight line segments between the shot points. Power spectral density estimates for the unfiltered data are shown in the inset. Cutoff half-wavelength for the filter was 50 km. Horizontal bars are interpreted horizontal extents of magnetic sources and numbers in parenthesis are estimated depths-to-sources. Distance scale is the same as figure 9.

11. With the exception of the anomaly at the southwest end of the profile (250-300 km on fig. 11), all the depths are about 30 km, at the top of the lower unit of the lower crust which we distinguish on the basis of the seismic data. We note that the shallower depth of 23 km for the anomaly at 170-259 km on fig. 11 could be explained by shallowing of the Curie point isotherm as the Red Sea is approached. Amplitudes of these anomalies are about 100 nT. Assuming a 30 km depth and the source to be the lowermost crustal layer of about 10 km thickness, the apparent susceptibility is 0.002-0.003 cgs, according to the models of Andreasen and Zietz (1969).

This result is in good agreement with those of Wasilewski and Fountain (1982) for laboratory determinations of the mean magnetization of the lower 10 km of crust in the Ivrea zone. In that work, Wasilewski and Fountain also determined that the Curie points of the magnetic minerals in the Ivrea arocks were in the range of 570-580°C. The inferred geotherms for the Arabian Shield (Gettings, 1982) are generally well below this value at the base of the crust, except to the southwest of shot point 4. Thus we conclude that there may be significant magnetic sources in the lowermost crust of the Shield. The anomalies at 570-650 km and 730-820 km (fig. 11) correlate with the gravity anomalies at the Najd fault zones there.

Structure of the lower crust

In our model the top of the lower crust is defined by a first order velocity discontinuity at a depth of 21 km across the entire profile from shot point 5 northeastward (fig. 3). Its base is the Mohorovicic discontinuity which occurs at about 38 km depth in the southwest and at approximately 43 km in the northeast part of the profile. We infer the discontinuity to be a large one in the northeastern half of the profile with a velocity increase from 7.3-7.4 km/s to 8.1 to 8.2 km/s. In the southwest part of the profile, the discontinuity is less marked with a velocity increase from 7.8 km/s to 8.0 km/s. We have used a linear gradient for the velocity-depth function in the lower crust with a change in slope at 29 km depth, which effectively divides the lower crust into two layers.

In this model (fig. 3) the boundaries which mark the top of the lower crust and divide it into two units continue across the Shield at a nearly constant depth, even though the velocities, densities, and magnetizations vary laterally by significant amounts. We interpret this relation as a horizontal zonation of metamorphic grades, increasing with depth, across the entire Shield. We thus conclude that the lateral variation of physical properties in the lower crust represents variations in average bulk composition. Southwest of

the Nabitah zone, where the velocity-depth function is in good agreement with that for the Ivrea zone (Fountain, 1976), we infer the bulk composition of the lower crust to be more mafic than to the northeast of the Nabitah zone. The approximate 10 km thickness and average velocity of 7.1-7.3 km/s of the lowermost crustal zone in our model are similar to the thickness and mean velocity of the granulite facies rocks in the Ivrea zone. To the northeast of the Nabitah zone, the systematically lower velocities are interpreted as indicating a more felsic bulk composition in both the upper and lower parts of the lower crust. In the extreme northeast, across the major lateral crustal discontinuity marking the boundary between continental blocks (see below), the lower crustal composition is probably again more mafic.

In summary, our model of the lower crust of southwestern Saudi Arabia is closely comparable with the Ivrea zone (Fountain, 1976) and is one in which there are lateral variations in bulk composition which are overprinted by metamorphism. Metamorphic grade decreases upward and we infer the rocks in the zone of the steepest velocity gradient from the Mohorovicic discontinuity to about 29 km depth to be in the granulite facies; above this level and below 21 km (the top of the lower crust) the rocks are inferred to be in the amphibolite facies. The facies boundary is probably transitional from amphibolites to granulites in the zone of velocity gradient change at about 29 km depth.

SOME SECOND-ORDER STRUCTURES

Basement configuration beneath the Arabian Platform

The extreme northeast end of the profile, which covers the transition between the Arabian Shield and the sedimentary rocks of the Arabian Platform, is of particular geological interest. The sediments of the platform in this region are mainly shale and sandstone in the lower half of the stratigraphic section and limestones and shales in the upper half (Powers and others, 1966). We used standard techniques to calculate the sedimentary thickness and the configuration of the basement beneath the sediments.

The basement structure derived from these observations is illustrated in figure 3. The model is based on the following assumptions: velocities of 3.09 and 6.15 km/s are appropriate for the sedimentary section and basement, respectively; dipping planar layers and vertical faults (horsts and grabens) are the structural elements of the basement. The model shows the sediments beginning at the edge of the Precambrian Shield at a distance of 43 km southwest of shot point 1. The sediments thicken to 600 m at shot point 1 and then dip at 1° to the northeast for 47 km, reaching a thickness of 1750 m. Beyond 47 km, the basement rises by 1000 m;

the width of the zone over which the basement rise occurs is known only to be less than the seismic station separation, 4 km at this point. This basement rise corresponds to a northwestward extension of a fault zone mapped by Bramkamp and Ramirez (1958). At a distance of 72 km from shot point 1 the basement drops to 1500 m, only to rise again to 750 m at 80 km. The basement structure between 70 and 80 km from shot point 1 appears to coincide with a southeastward extension of a mapped fault zone and graben system (Bramkamp and Ramirez, 1958).

A significant increase in high frequencies at a range of 43 km southwest of shot point 1 was observed in the seismograms indicating that the average attenuation of the high frequencies decreases sharply beyond 43 km southwest of shot point 1; the termination of the sediments, which attenuate the high frequency components of the seismograms, is the obvious explanation.

Variations in depth to the basement beneath the sediments of the Arabian Platform near shot point 1 coincide with mapped fault zones associated with the Central Arabian Arch. The basement structures are thus probably horsts and grabens rather than a paleoerosional surface, with vertical relief on the order of 1000 m.

Lateral crustal discontinuity at the northeast end of the seismic profile

We identify a lateral crustal boundary 30 km northeast of shot point 2 across which velocities increase to the northeast by about 0.2 km/s. These relatively high upper crustal velocities (6.3-6.5 km/s) may be attributed to the higher average metamorphic grade of these rocks, and the velocity change indicates that the crust here is different from that to the west, as suggested by Schmidt and others (1978). We note that northeast of the boundary the lower crustal velocities below 30 km depth increase along a smaller gradient than along other portions of the profile. The boundary zone, as seismically determined, is about 40 km southwest along the profile of the Al Amar-Idsas fault, which has been commonly accepted (Schmidt and others, 1978) as marking the western edge of an allochthonous continental block. The uncertainty of the location of the seismic velocity boundary is about ±15 km; therefore, it occurs at least 25 km southeast along the profile of the Al Amar-Idsas fault. Delfour (1979) has suggested that the Abt schist formation, which extends from the Al Amar-Idsas fault southwest to the seismic boundary, may contain unidentified thrust faults; an imbricate structure for the Precambrian collision zone (Schmidt and others, 1978) would explain the displacement of the seismically-determined zone from the Al Amar-Idsas fault. The refraction data at this level of interpretation cannot resolve the dip

of the zone or even its direction, so we have drawn it vertically in fig. 3, as we have drawn all other zones between laterally-inhomogenous portions of the crust.

Seismic characteristics of the Shammar and Najd tectonic provinces

We cannot distinguish the southwest part of the Shammar tectonic province from the Najd province because of a lack of data from shot point 3 northeast; the crustal structure is undoubtedly more complicated than figure 3 represents. The velocities observed are typical of those in crystalline upper crustal rocks. However, the lower crustal velocities (20-40 km depth) are anomalously high and atypical of granitic crust; they are more indicative of a mafic crust. The evolutionary models of Schmidt and others (1978) involve crustal formation from collisions of island arc systems and imply such bulk compositions.

At the southwest Najd fault zone, which delimits the southwest boundary of the Najd tectonic province (between 35 and 80 km southwest of shot point 3) there is a lateral seismic discontinuity across which uppermost crustal velocities change from 6.1 km/s in the northeast to 6.3 km/s in the southwest. The high-velocity region apparently includes the fault zone and we interpret the portion beneath the fault zone as a velocity discontinuity at 13 km depth. As discussed above, this high-velocity zone correlates well with the gravity anomaly highs and strong magnetic anomalies. Estimates of the depth to the center of mass from gravity anomalies are 15-20 km and assuming that the seismic discontinuity at 13 km depth marks the top of the source, we interpret this zone as one of mafic intrusions into the fault zone at lower crustal levels.

On the basis of gravity and magnetic evidence discussed above, we postulate that the northeast Najd fault zone also has an analogous zone of intrusions beneath it with associated intracrustal velocity discontinuity at ~13 km depth. There is no data coverage in the record section northeast of shot point 3, and southwest from shot point 2 the zone in question is too far away to be detected as a reflector. Thus the existance of the reflector is speculative.

Velocity structure of the Hijaz-Asir tectonic province

Approximately 100 km southwest of shot point 3, a lateral velocity boundary occurs in the lower crust, with the lower velocities to the southwest. This low-velocity lower crust begins beneath the Nabitah suture zone mapped at the surface (Schmidt and others, 1978) and extends for about 220 km, to about 70 km southwest of shot point 4. It may correspond to the remnants of the upper part of a subducted plate hypothe-

sized by Schmidt and others (1978). In the upper crust, the high-velocity zone that began at the southwest Najd fault zone continues across the Al Qarah gneiss domes (Schmidt and others, 1978) to the Al Junaynah fault zone, which is about 30 km northeast of shot point 4. Between the Al Junaynah fault zone and a point about 65 km northeast of shot point 4, another 13 km-deep seismic discontinuity is inferred, at a depth corresponding to the lower regions of the Al Qarah gneiss dome (Schmidt and others, 1978).

In the uppermost crust, a lateral velocity discontinuity is seen in the vicinity of shot point 4, at the Al Junaynah fault zone. Velocities are lower to the southwest, 6.2 km/s, for about 60 km. They increase dramatically approaching the Khamis Mushayt gneiss (Coleman, 1973), reaching 6.6 km/s at depths of only 5 km in the core of the gneiss (fig. 3). The high-velocity region, which correlates closely with the outcrop pattern of the Khamis Mushaytt gneiss, appears to penetrate the entire upper crust. This may be the best geophysical example along the profile of a nappe-type structure, in which lower crustal material has been brought to the present-day surface. The velocity structure of the lower crust beyond about 80 km southwest of shot point 4 are comparable to velocities found between shot points 3 and 2. Upper mantle velocities, however, seem to be systematically lower by about 0.2 km/s than those to the northeast.

The seismic data along the profile show strong variations in seismic wave attentuation Q. The large, batholithic-size granitoid bodies, particularly the gneiss dome areas, have a very high Q; that is, they propagate seismic energy very efficiently. In general, the traces recorded at stations on these rocks have high amplitudes and large relative high-frequency content. For stations on greenstone and greenschist and at the large fault zones, the Q is much lower, and the higher frequencies are generally lost. Higher Q and higher upper-crustal velocities seem to be related to higher metamorphic grade, therefore detailed correlations between the true-amplitude record sections and geologic maps at 1:100,000 and 1:250,000 scales may assist in mapping metamorphic grade changes along the profile.

Bulk magnetization of upper crustal blocks

Three intervals of the digitized aeromagnetic profile were used to investigate the relative intensities of bulk magnetization of crustal blocks defined by lateral velocity discontinuities. Since the total intensity profile was used, the resulting power spectra will reflect mainly upper crustal sources and thus can be regarded as comparing the magnetization of upper crustal blocks. The intervals were (see fig. 3): (1) 220-320 km, sampling the central part of the Hijaz-Asir tectonic province; (2) 400-570 km, sampling the north-

east part of the Hijaz-Asir province in the area of the Al Qarah gneiss dome; and (3) 570-780 km, sampling the Najd tectonic province. Power spectral density estimates for these three segments are shown in figure 12. It is immediately obvious that the bulk magnetization is substantially higher for the segment including the Al Qarah gneiss dome than for either of the other segments. The two other segments have very similar spectra, and the magnetic rocks of these provinces are predominantly greenstone and greenschist. Since the bulk magnetization of rocks of the greenschist facies is generally considerably lower than those of higher grade facies we presume that the higher metamorphic grade of the block with the Al Qarah gneisses is the explanation of its higher magnetization. We note that this block also has a higher average velocity, in agreement with the postulated higher average metamorphic grade.

SUMMARY

On the basis of seismic deep-refraction, regional gravity, aeromagnetic and heat flow data, we have formulated an initial crustal model for the southern Red Sea and Arabian Plate. From the plate tectonic standpoint, we have assumed that the Red Sea-Arabian Plate system is driven by a convective system in the aesthenosphere in which hot material is upwelling beneath the axis of the Red Sea and flowing laterally to the northeast below the Arabian Plate. The lithosphere has been heated by the underlying aesthenosphere, resulting in a regional uplift of the entire system which exceeds 3 km at the passive margin between the Arabian Shield and the Cenozoic rocks of the Red Sea basin and decreases gradually to about zero at the Arabian Gulf. The seismic refraction data imply upper mantle compressional wave velocities which increase uniformly from 8.0 km/s beneath the Red Sea and southwestern Shield to 8.2 km/s beneath the Arabian Platform, while the depth to the Mohorovicic discontinuity beneath the Shield increases from about 38 km in the southwest to 43 km in the northeast. Two deeper velocity discontinuities have been distinguished, one at 59 km and one at 70 km depth in the upper mantle. The regional gravity anomaly pattern, when geometrically constrained by the seismic refraction data, requires a steady increase in density of the upper mantle rocks to the northeast. The heat flow data show a gradual increase to the southwest, and analysis of the deep-source components of the aeromagnetic field suggests that the depth to the Curie-point isotherm decreases southwestward across the Shield. All of these data support the hypothesized mechanism of uplift.

The boundary zone at the southwestern edge of the Shield is approximately in the middle of a steep Bouguer gravity anomaly gradient which decreases from positive anomaly values in the southwest to strongly negative values to

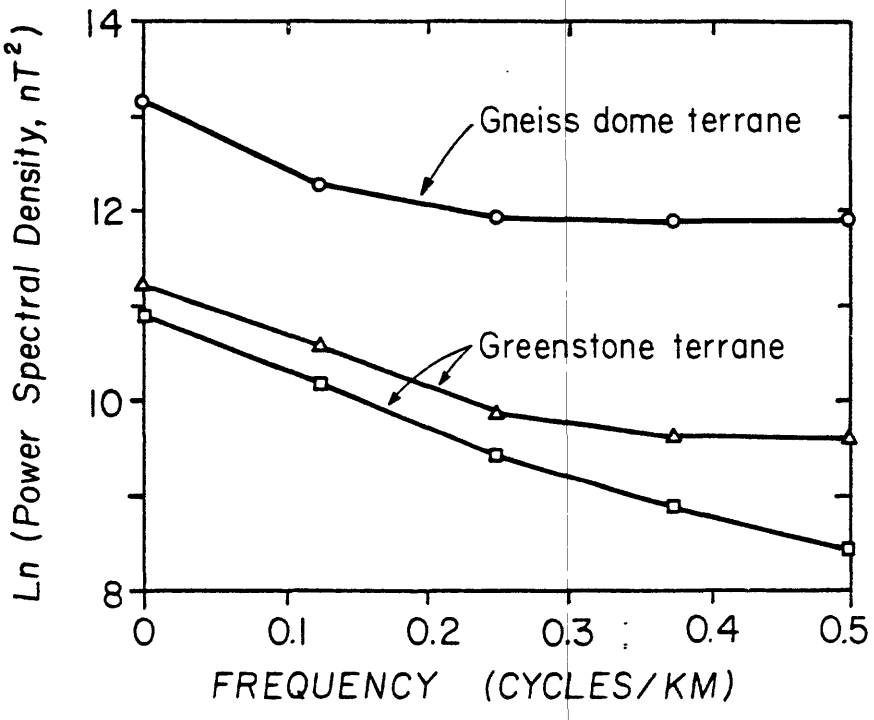

Figure 12.--Estimates of power spectral density for three segments of the aeromagnetic profile. Square symbols are for the 220-320 km interval on the profile in the Hijaz-Asir tectonic province consisting mainly of mafic greenstones and greenschists. Open circles are for the 400-570 km interval sampling the Al Qarah gneiss dome terrane and nearby rocks, and the open triangles are for the 570-780 km interval of the profile that samples the Najd tectonic province (andesitic greenstone and greenschist). The systematically larger power at all frequencies for the gneiss dome province implies a larger bulk magnetization for the gneisses than for the greenschist facies rocks.

the northeast over the Shield. The zone is characterized by an increasing volume proportion of diabase dikes southwestward from the outcrops of Shield rocks and has seismic velocities within the range of those measured for diabase. The seismically determined thickness of the crust thins from about 16 km at the boundary zone to 8 km beneath the Farasan Islands. The velocity-depth function inferred for the Red Sea shelf from the refraction data shows good agreement with velocity-depth functions inferred from measurements of samples of the Samail ophiolite in Oman. The aeromagnetic field over the boundary zone and southwestward has the characteristic striped pattern of sea-floor crust, and the heat flow values at the boundary and over the shelf areas are anomalously high. On these bases, we believe that the coastal plain and shelf are underlain by oceanic crust created by sea-floor spreading processes, probably within the last 20 Ma, and that at least in this portion of the Red Sea, the oceanic crust extends very nearly to the exposed edge of Precambrian outcrop. Both the gravity data and the seismic refraction data indicate that the crust thickens abruptly northeast of this boundary zone to the normal Shield thickness of about 40 km.

On the Arabian Shield, the seismic refraction data show two nearly horizontal velocity discontinuities which persist across the entire Shield, one at about 20 km depth and the other at about 30 km depth. As a result of comparisons of velocity-depth functions from the seismic refraction data on the Shield with measured velocities of rocks from the Ivrea zone in northern Italy, the horizontal velocity stratification is interpreted to represent metamorphic grade changes. Thus, the upper crust, from the surface to about 20 km depth, is associated with the greenschist facies, the layer from 20 to 30 km depth is identified with the amphibolite facies, and the lowermost crust, from 30 to 40 km depth, may represent the granulite-eclogite facies.

A number of lateral seismic velocity discontinuities in the crust of the Shield have been identified from the seismic refraction data. Since these discontinuities can generally be shown to correspond with changes in the gravity anomaly and aeromagnetic fields, we interpret them as changes in bulk composition of the rocks of the layer with the discontinuity. The major lateral crustal discontinuity in both the upper and lower crust intersects the profile about 25 km northeast of shot point 2. Crustal velocities generally increase across this boundary to the northeast by about 0.2 km/s. This boundary is substantially west of the Al Amar-Idsas fault, which is generally regarded as a suture zone between two Precambrian blocks (Schmidt and others, 1978). We infer that the actual crustal boundary is the seismically-defined one and that the Al Amar-Idsas zone may be one of a series of imbricate thrust faults that are the surface expression of

the suture. The suture zone apparently extends from the Al Amar-Idsas fault almost to shot point 2. In any case, the seismic refraction data support the hypothesis that the two blocks of crust are quite different.

In the lower crust of the Shield southwest of shot point 3, we distinguish a zone of average velocity about 6.9 km/s that extends from beneath the Nabitah fault zone southwest along the profile for about 200 km. To the southwest of this zone the lower crust has an average velocity about 7.0 km/s. If the models of crustal evolution of Schmidt and others (1978) are correct, this lower crustal block of 6.9 km/s material may represent the remnants of the upper part of a subducted plate.

We have identified a distinctive, high-velocity anomaly in the upper crust of the Shield, about midway between shot points 4 and 5 that correlates well with the outcrop of high-grade gneisses and amphibolites of the Khamis Mushayt gneiss of Coleman (1973) and with a level shift in the Bouguer gravity anomaly field to less negative anomaly values. The velocity anomaly, which is probably the seismic expression of this extensive gneiss dome or batholithic structure, apparently penetrates the entire upper crust. A similar, although less pronounced, velocity anomaly and corresponding gravity anomaly high occurs between the Al Junaynah and Nabitah fault zones; it correlates with the Al Qarah gneiss dome of Schmidt and others (1978).

Upper crustal average velocities are higher to the southwest of the southern Najd fault zone than to the northeast which probably reflects the more mafic average composition of the volcanic rocks southwest of the Nabitah fault zone. Two intracrustal reflectors that have been identified at a depth of about 13 km beneath the Al Junaynah and southwestern Najd fault zones have pronounced gravity anomaly highs associated with them and the reflectors probably indicate the upper limits of extensive mafic intrusive activity within the zones.

The seismic refraction data show that the basement surface beneath the sediments of the platform at the northeast end of the profile appears to be faulted in a horst and graben pattern northeast of shot point 1 on extensions of fault zones mapped at the surface. Offsets due to faulting are of the order of 1000 m, and the maximum sediment thickness is about 1.75 km.

In summary, we have presented a model of the Arabian Shield that is composed of several island arcs after collision and that is more mafic in average composition than some other Shields. The Arabian Shield abuts a modern day seafloor spreading system and the Red Sea-Arabian Plate system is underlain by an actively convecting aesthenosphere. We have shown that this model satisfies in a regional sense the constraints of the available geologic, seismic, gravity, heat flow, and aeromagnetic data.

DATA STORAGE

No base data files were established as a result of this study and no entries or updates were made to the Mineral Occurrence Documentation System (MODS) data bank.

REFERENCES CITED

Abdel-Gawad, M., 1970, Interpretation of satellite photographs of the Red Sea and Gulf of Aden: Philosophical Transactions of the Royal Society of London, ser. A, v. 264, p. 23–40.

Aldrich, L. T., Brown, G. F., Hedge, Carl, and Marvin, Richard, 1978, Geochronologic data for the Arabian Shield, Sec. 1 - Radiometric age determinations of some rocks from the Arabian Shield, by L. T. Aldrich, Sec. 2 - Tabulation of Rb-Sr and K-Ar ages given by rocks of the Arabian Shield, by G. F. Brown, Carl Hedge, and Richard Marvin: U.S. Geological Survey Saudi Arabian Project Report 240, 20 p.

Andreasen, G. E., Petty, A. J., and Blank, H. R., 1980, Total-intensity aeromagnetic map of the Precambrian Arabian Shield, Kingdom of Saudi Arabia: Saudi Arabian Directorate General of Mineral Resources, scale 1:2,000,000. Special edition for the 26th International Geological Congress, Paris, 1980.

Andreasen, G. E., and Petty, A. J., 1973, Total intensity aeromagnetic map of the Southern Najd quadrangle and part of the Southern Tuwayq quadrangle, Kingdom of Saudi Arabia: Saudi Arabian Directorate General of Mineral Resources Geologic Map GM-13, 3 p., scale 1:500,000.

Andreasen, G. E., and Petty, A. J., 1974a, Total intensity aeromagnetic map of the Wadi ar Rimah Quadrangle and part of the Northern Tuwayq quadrangle, Kingdom of Saudi Arabia: Saudi Arabian Directorate General of Mineral Resources Geologic Map GM-11, 3 p., scale 1:500,000.

Andreasen, G. E., and Petty, A. J., 1974b, Total intensity aeromagnetic map of the Thiamat ash Sham quadrangle and part of the Asir quadrangle, Kingdom of Saudi Arabia: Saudi Arabian Directorate General of Mineral Resources Geologic Map GM-14, 3 p., scale 1:500,000.

Andreasen, G. E., and Zietz, Isadore, 1969, Magnetic fields for a 4 x 6 prismatic model: U.S. Geological Survey Professional Paper 666, 9 p., 210 pl.

Bartov, Y., Steinitz, G., Eyal, M., and Eyal, Y., 1980, Sinistral movement along the Gulf of Aqaba - its age and relation to the opening of the Red Sea: Nature, v. 285, no. 5762, p. 220-221.

Baubron, J. C., Delfour, J., and Vialette, Y., 1976, Geochronological measurements (Rb/Sr; K/Ar) on rocks of the Arabian Shield: Bureau de Recherches Geologiques et Minieres (Saudi Arabian Mission) Report 76-JED-22, 152 p.

Blank, H. R., Jr., 1977, Aeromagnetic and geologic study of Tertiary dikes and related structures of the Arabian margin of the Red Sea: In Red Sea Research 1970-1975: Saudi Arabian Directorate General of Mineral Resources Bulletin 22, p. G1-G18.

Blank, H. R., Healy, J. H., Roller, J., Lamson, R., Fisher, F., McLearn, R., and Allen S., 1979, Seismic refraction profile, Kingdom of Saudi Arabia-field operations, instrumentation, and initial results: U.S. Geological Survey Open-File Report 79-1568, (IR)SA-259.

Blank, H. R., Gettings, M. E., and Kellogg, K. S., 1981, Linear magnetic anomalies onshore and offshore in southwest Saudi Arabia (abs.): EOS, American Geophysical Union Transactions, v. 62, no. 17, p. 407.

Bramkamp, R. A., and Ramirez, L. F., 1958, Geologic map of the Northern Tuwayq quadrangle, Kingdom of Saudi Arabia: U.S. Geological Survey Miscellaneous Geologic Investigations Map I-207A, scale 1:500,000.

Brown, G. F., 1970, Eastern margin of the Red Sea and the coastal structures in Saudi Arabia: Philosophical Transactions of the Royal Society of London, Ser. A, v. 267, p. 75-87.

Brown, G. F., 1972, Tectonic map of the Arabian Peninsula: Saudi Arabian Directorate General of Mineral Resources Arabian Peninsula Map AP-2, scale 1:4,000,000.

Aldrich, L.T., Brown, G.F., Hedge, C.E., and Marvin, Richard, 1978, Geochronologic data for the Arabian Shield, sec. 2 -Tabulation of Rb-Sr and K-Ar ages given by rocks of the Arabian Shield: U.S. Geological Survey

Brown, G. F., and Jackson, R. O., 1960, The Arabian Shield: International Geological Congress, 21st, Copenhagen, 1960, Proceedings, sec. 9, p. 69-77.

Brown, G. F., and Jackson, R. O., 1978, An overview of the geology of western Arabia: King Abdulaziz University Institute of Applied Geology Symposium on Evolution and Mineralization of the Arabian-Nubian Shield, Proc. I.A.P. Bull. 3, v. 1, p. 3-10.

Christensen, N. I., and Smewing, J. D., 1981, Geology and seismic structure of the northern section of the Oman Ophiolite: Journal of Geophysical Research, v. 86, no. B4, p. 2545-2556.

Coleman, R. G., 1973, Reconnaissance geology of the Khaybar quadrangle, Kingdom of Saudi Arabia: Saudi Arabian Directorate General of Mineral Resources Geologic Map GM-4, 5 p., scale 1:100,000.

Coleman, R. G., Brown, G. F., and Keith, T. E. C., 1972, Layered gabbros in southwest Saudi Arabia: U.S. Geological Survey Professional Paper 800-D, p. D143-D150.

Cooper, J. A., Stacey, J. S., Stoeser, D. B., and Fleck, R. J., 1979, An evaluation of the zircon method of isotopic dating in the southern Arabian craton, Kingdom of Saudi Arabia: U.S. Geological Survey Open-File Report 79-1107, (IR)SA-257.

Delfour, J., 1979, Geologic map of the Halaban quadrangle, sheet 23G, Kingdom of Saudi Arabia (with topographic base): Saudi Arabian Directorate General of Mineral Resources Geologic Map GM-46A, scale 1:250,000.

Dodge, F. C. W. 1979, The Uyaijah ring structure, Kingdom of Saudi Arabia: U.S. Geological Survey Professional Paper 774-E, 17 p.

Drake, C. L. and Girdler, R. W., 1964, A geophysical study of the Red Sea: Geophysical Journal of the Royal Astronomical Society, v. 8, p. 473-495.

Eaton, J. P., O'Neill, M. E., and Murdock, J. N., 1970, Aftershocks of the 1966 Parkfield-Cholame, California, earthquake: a detailed study: Bulletin of the Seismological Society of America, v. 60, p. 1151-1197.

Fleck, R. J., Greenwood, W. R., Hadley, D. G., Anderson, R. E., and Schmidt, D. L., 1979, Rubidium-strontium geochronology and plate tectonic evolution of the southern part of the Arabian Shield: King Abdulaziz University, Institute of Applied Geology Bull. 3, v. 3, Pergamon Press, Oxford-New York, p. 1-18.

Fleck, R. J., Coleman, R. G., Cornwall, H. R., Greenwood, W. R., Hadley, D. G., Schmidt, D. L., Prinz, W. C., and Ratte, J. C., 1976, Geochronology of the Arabian Shield, Western Saudi Arabia; K-Ar results: Bulletin of the Geological Society of America, v. 87, p. 9-21.

Fountain, D. M., 1976, The Ivrea-Verbano and Strona-Ceneri zones, northern Italy: a cross-section of the continental crust; new evidence from seismic velocities of rock samples: Tectonophysics, v. 33, p. 145-165.

Freund, R., Garfunkel, Z., Zak, I., Goldberg, M., Weissbrod, T., and Derin, B., 1970, The shear along the Dead Sea Rift: Philosophical Transactions of the Royal Society of London, Ser. A, v. 267, p. 107-130.

Freund, R., Zak, I., and Garfunkel, Z., 1968, Age and rate of the sinistral movement along the Dead Sea rift: Nature, v. 220, p. 253-255.

Gettings, M. E., 1977, Delineation of the continental margin in the southern Red Sea region from new gravity evidence; in Red Sea Research 1970-1975: Saudi Arabian Directorate General of Mineral Resources, Bulletin 22, p. K1-K11.

Gettings, M. E., 1981, A heat flow profile across the Arabian Shield and Red Sea (abs.): EOS, Transactions of the American Geophysical Union, v. 62, no. 17, p. 407.

Gettings, M. E., 1982, Heat flow measurements at the 1978 Saudi Arabia deep-seismic refraction line shot points II. Discussion and interpretation: Saudi Arabian Deputy Ministry for Mineral Resources Open-File Report USGS-OF-02-40, 40 p.

Gettings, M. E., 1983, A simple Bouguer gravity anomaly map of southwestern Saudi Arabia and an initial interpretation: Saudi Arabian Deputy Ministry for Mineral Resources Open-File Report (U.S. Geological Survey Saudi Arabian Mission), 63 p.

Gettings, M. E., and Showail, Abdullah, 1982, Heat flow measurements at the 1978 Saudi Arabian deep-refraction line, Part 1: Results of the measurements: Saudi Arabian Deputy Ministry for Mineral Resources Open-File Report USGS-OF-02-39, 98 p. : also, 1982, U.S. Geological Survey Open-File Report 82-794.

Ghent, E. D., Coleman, R. G., and Hadley, D. G., 1980, Ultramafic inclusions and host alkalai olivine basalts of the southern coastal plain of the Red Sea, Saudi Arabia: American Journal of Science, v. 280A, p. 499-527.

Gillmann, M., 1968, Primary results of a geological and geophysical reconnaissance of the Jizan coastal plain in Saudi Arabia: American Institute of Mining and Metallurgical Engineers, Society of Petroleum Geologists, Saudi Arabian Section, 2nd Regional Symposium, Dhahran, Proceedings, p. 189-208.

Girdler, R. W., 1969, The Red Sea: a geophysical background, in Degens, E. T., and Ross, D. A., eds., Hot brines and recent heavy metal deposits in the Red Sea: New York, Springer-Verlag, p. 38-58.

Girdler, R. W ., 1970, A review of Red Sea heat flow: Philosophical Transactions of the Royal Society of London, Ser. A, v. 267, p. 191-203.

Girdler, R. W., and Evans, T. R., 1977, Red Sea heat flow: Geophysical Journal of the Royal Astronomical Society, v. 51, no. 1, p. 245-251.

Girdler, R. W., and Styles, P., 1974, Two stage Red Sea floor spreading: Nature, v. 247, p. 7-11.

Greenwood, W. R., and Anderson, R. E., 1977, Palinspastic map of the Red Sea area prior to Miocene sea floor spreading in Red Sea Research 1970-1975: Saudi Arabian Directorate General of Mineral Resources Bulletin 22, p. Q1-Q6.

Greenwood, W. R., Anderson, R. E., Fleck, R. J., and Roberts, R. J., 1977, Precambrian geologic history and plate tectonic evolution of the Arabian Shield: Saudi Arabian Directorate General of Mineral Resources Bull. 24, 35 p.

Hadley, D. G., and Schmidt, D. L., 1979, Proterozoic sedimentary rocks and basins of the Arabian Shield and their evolution: U.S. Geological Survey Open-File Report 79-1189, (IR)SA-242.

Hall, S. A., 1980, A total intensity magnetic anomaly map of the Red Sea and its interpretation: U.S. Geological Survey Open-File Report 80-131, (IR)SA-275.

Hall, S. A., Andreasen, G. E., and Girdler, R. W., 1976, Total-intensity magnetic anomaly map of the Red Sea and adjacent coastal areas: Saudi Arabian Directorate General of Mineral Resources Bull. 22, p. F1-F15.

Healy, J. H., Mooney, W. D., Blank, H. R., Gettings, M. E., Kohler, W. M., Lamson, R. J., Leone, L. E., 1982, Saudi Arabian seismic deep-refraction profile: final project report: Saudi Arabian Deputy Ministry for Mineral Resources Open-File Report USGS-OF-02-37, 429 p., also, 1983, U.S. Geological Survey Open-File Report 83-390.

Hill, M. N., 1957, Recent geophysical exploration of the ocean floor; in Ahrens, L. H., and others, eds., Physics and chemistry of the Earth, v. 2: New York, Pergamon, p. 129-163.

Jackson, R. O., Bogue, R. G., Brown, G. F., and Gierhart, R. D., 1963, Geologic map of the southern Najd quadrangle, Kingdom of Saudi Arabia: U.S. Geological Survey Miscellaneous Geologic Investigations Map I-211A, scale 1:500,000.

Jones, A. G., 1981, On a type classification of lower crustal layers under Precambrian regions: Journal of Geophysics, v. 49, p. 226-233.

Kellogg, K. S., and Blank, H. R., 1982, Paleomagnetic evidence bearing on Tertiary tectonics of the Tihamat Asir coastal plain, southwestern Saudi Arabia: Saudi Arabian Deputy Ministry for Mineral Resources Open-File Report USGS-OF-02-65, 37 p.: also, 1982, U.S. Geological Survey Open-File Report 82-1047.

Knopoff, L., and Fouda, A. A., 1975, Upper-mantle structure under the Arabian Peninsula: Tectonophysics, v. 26, no. 1-2, 121-134.

Knott, S. T., Bunce, E. T., and Chase, R. L., 1966, Red Sea seismic reflection studies: Canada Geological Survey Paper 66-14, p. 33-61.

Kohn, B. P., and Eyal, M., 1981, History of uplift of the crystalline basement of Sinai and its relation to opening of the Red Sea as revealed by fission track dating of apatites: Earth and Planetary Science Letters, v. 52, p. 129-141.

Lachenbruch, A. H., 1970, Crustal temperature and heat production: implications of the linear heat-flow relation: Journal of Geophysical Research, v. 75, no. 17, p. 3291-3300.

Laughton, A. S., 1970, A new bathymetric chart of the Red Sea: Philosophical Transactions of the Royal Society of London, Ser. A, v. 267, p. 21-22.

Le Pichon, Xavier, Francheteau, Jean, and Bonnin, Jean, 1973, Plate Tectonics 2nd ed.: Amsterdam, Elsevier, 311 p.

Nafe, J. E., and Drake, C. L., 1968, Physical properties of rocks of basaltic composition, in Hess, H. H., and Poldervaart, A., eds., Basalts: the Poldervaart treatise on rocks of basaltic composition, v. 2: New York, Interscience, p. 483-502.

Niazi, M., 1968, Crustal thickness in the Saudi Arabian Peninsula: Geophysical Journal of the Royal Astronomical Society, v. 15, no. 5, p. 545-547.

Noy, D. J., 1978, A comparison of magnetic anomalies in the Red Sea and the Gulf of Aden: in Tectonics and Geophysics of Continental Rifts: NATO Advanced Study Institute Series, Ser. C, v. 37, p. 279-287.

Phillips, J. D., 1970, Magnetic anomalies in the Red Sea: Philosophical Transactions of the Royal Society of London, ser. A, v. 267, p. 205-217.

Phillips, J. D., and Ross, D. A., 1970, Continuous seismic reflection profiles in the Red Sea: Philosophical Transactions of the Royal Society of London, ser. A, v. 267, p. 143-152.

Powers, R. W., Ramirez, L. F., Redmond, C. D., and Elberg, E. L., Jr., 1966, Geology of the Arabian Peninsula -sedimentary geology of Saudi Arabia: U.S. Geological Survey Professional Paper 560-D, 147 p.

Quennell, A. M., 1958, The structural and geomorphic evolution of the Dead Sea rift: Quarterly Journal of the Geological Society of London, v. 114, p. 1-24.

Raitt, R. W., 1963, The crustal rocks, in Hill, M. N., ed., The sea, v. 3: New York, Interscience, p. 85-102.

Ramsay, C. R., Jackson, N. J. and Roobol, M. J., 1979, Structural/lithologic provinces in a Saudi Arabian Shield geotraverse, in Evolution and Mineralization of the Arabian-Nubian Shield, v. 1: Oxford-New York, Pergamon Press, p. 64-84, (King Abdulaziz University, Institute of Applied Geology, I.A.G. Bulletin no. 3, v. 1).

Roeser, H. A., 1975, A detailed magnetic survey of the southern Red Sea: Geologisches Jahrbuch, Reihe D. No. 13, p. 131-153.

Schmidt, D. L., Hadley, D. G., Greenwood, W. R., Gonzalez, L., Coleman, R. G., and Brown, G. F., 1973, Stratigraphy and tectonism of the southern part of the Precambrian Shield of Saudi Arabia: Saudi Arabian Directorate General of Mineral Resources Bulletin No. 8, 13 p.

Schmidt, D. L., Hadley, D. G., and Stoeser, D. B., 1979, Late Proterozoic crustal history of the Arabian Shield, Southern Najd province, Kingdom of Saudi Arabia, in Evolution and mineralization of the Arabian-Nubian Shield: King Abdulaziz University, Institute of Applied Geology Bulletin 3, v. 2: Pergamon Press, Oxford-New York, p. 41-58.

Stacey, J. S., Delevaux, M. H., Gramlich, J. W., Doe, B. R., and Roberts, R. J., 1981, A lead-isotope study of mineralization in the Arabian Shield: U.S. Geological Survey Saudi Open-File Report 81-193, (IR)SA-347.

Stoeser, D. B., and Elliott, J. E., 1979, Post-orogenic peralkaline and calc-alkaline granites and associated mineralization of the Arabian Shield, Kingdom of Saudi Arabia: U.S. Geological Survey Open-File Report 79-1323, (IR)SA-265.

Talwani, Manik, Worzel, J. L., Landisman, M. G., 1959, Rapid gravity computations for two-dimensional bodies with application to the Mendocino submarine fracture zone: Journal of Geophysical Research, v. 64, 49-59.

Tramontini, C., and Davies, D., 1969, A seismic refraction survey in the Red Sea: Geophysical Journal of the Royal Astronomical Society, v. 17, p. 225-241.

U.S. Geological Survey and Arabian-American Oil Company, 1963, Geologic map of the Arabian Peninsula: U.S. Geological Survey Miscellaneous Geologic Investigations Map I-270A, scale 1:2,000,000.

Vine, F. J., 1966, Spreading of the ocean floor--new evidence: Science, v. 154, p. 1405-1415.

Wasilewski, Peter, and Fountain, D. M., 1982, The Ivrea Zone as a model for the distribution of magnetization in the continental crust: Geophysical Research Letters, v. 9, no. 4, p. 333-336.

Wegener, Alfred, 1920, Die entstehung der kontinente and ozeane: Braunschwieg, F. Vieweg und Sohn, 135 p.